U.S. DEPARTMENT OF COMMERCE
National Technical Information Service

PB-264 495

Measurement of Dry Deposition of Fossil Fuel Plant Pollutants

Battelle Pacific Northwest Labs, Richland, Wash

Prepared for

Environmental Sciences Research Lab, Research Triangle Park, N C

Nov 76

TECHNICAL REPORT DATA
(Please read Instructions on the reverse before completing)

1. REPORT NO.
EPA-600/4-76-056

2.

3. RECIPIENT'S ACCESSION NO.

4. TITLE AND SUBTITLE
MEASUREMENT OF DRY DEPOSITION OF FOSSIL FUEL PLANT POLLUTANTS

5. REPORT DATE
November 1976

6. PERFORMING ORGANIZATION CODE

7. AUTHOR(S)
J. G. Droppo, D. W. Glover, A. B. Abbey, C. W. Spicer, and J. Cooper

8. PERFORMING ORGANIZATION REPORT NO.

9. PERFORMING ORGANIZATION NAME AND ADDRESS
Battelle-Pacific Northwest Laboratories
Battelle Boulevard
Richland, Washington 99352

10. PROGRAM ELEMENT NO.
1AA009

11. CONTRACT/GRANT NO.
68-02-1747

12. SPONSORING AGENCY NAME AND ADDRESS
Environmental Sciences Research Laboratory
Office of Research and Development
Environmental Protection Agency
Research Triangle Park, NC 27711

13. TYPE OF REPORT AND PERIOD COVERED
Final 6/24/74-6/24/76

14. SPONSORING AGENCY CODE
EPA/600/09

15. SUPPLEMENTARY NOTES

16. ABSTRACT

Dry removal of air pollutants from fossil fuel plants is considered from both a modeling and measurement viewpoint. Literature on dry deposition rates is summarized and the processes involved in dry deposition are discussed. The dry deposition of SO_2, O_3, NO_x, and NO, as well as total sulfur and lead particles are considered.

A prototype field data acquisition system was developed, assembled, and tested. Deposition velocities were computed for each field test.

The sulfur dioxide profiles gave reasonable estimates of the dry deposition values, comparable to those in the literature. They varied from 0.10 to 2.38 cm/sec for the test runs. Values for the O_3 deposition velocities were very small. The results for NO varied over a wide range, with the number of profiles measured in the test runs insufficient for reaching a definitive conclusion.

17. KEY WORDS AND DOCUMENT ANALYSIS

a. DESCRIPTORS	b. IDENTIFIERS/OPEN ENDED TERMS	c. COSATI Field/Group
*Mathematical Models Reaction Kinetics Electric Power Plants Air Pollution		12A 07D 10B 13B

18. DISTRIBUTION STATEMENT
RELEASE TO PUBLIC

19. SECURITY CLASS *(This Report)*
UNCLASSIFIED

20. SECURITY CLASS *(This page)*
UNCLASSIFIED

21. NO. OF PAGES
135

22. PRICE

EPA Form 2220-1 (9-73)

PB 264 495

EPA-600/4-76-056
November 1976

Environmental Monitoring Series

UNITED STATES
ENVIRONMENTAL PROTECTION AGENCY

REPRODUCED BY
NATIONAL TECHNICAL
INFORMATION SERVICE
U. S. DEPARTMENT OF COMMERCE
SPRINGFIELD, VA. 22161

RESEARCH REPORTING SERIES

Research reports of the Office of Research and Development, U.S. Environmental Protection Agency, have been grouped into five series. These five broad categories were established to facilitate further development and application of environmental technology. Elimination of traditional grouping was consciously planned to foster technology transfer and a maximum interface in related fields. The five series are:

1. Environmental Health Effects Research
2. Environmental Protection Technology
3. Ecological Research
4. Environmental Monitoring
5. Socioeconomic Environmental Studies

This report has been assigned to the ENVIRONMENTAL MONITORING series. This series describes research conducted to develop new or improved methods and instrumentation for the identification and quantification of environmental pollutants at the lowest conceivably significant concentrations. It also includes studies to determine the ambient concentrations of pollutants in the environment and/or the variance of pollutants as a function of time or meteorological factors.

This document is available to the public through the National Technical Information Service, Springfield, Virginia 22161.

EPA-600/4-76-056
November 1976

MEASUREMENT OF DRY DEPOSITION
OF FOSSIL FUEL PLANT POLLUTANTS

By

J. G. Droppo, D. W. Glover and O. B. Abbey
Battelle, Pacific Northwest Laboratory
Richland, Washington 99352

C. W. Spicer
Battelle, Columbus Laboratories
Columbus, Ohio 43201

John Cooper
ORTEC
Oak Ridge, Tennessee 37830

Contract No. 68-02-1747

Project Officer
Herbert J. Viebrock
Meteorology and Assessment Division
Environmental Sciences Research Laboratory
Research Triangle Park NC 27711

U.S. ENVIRONMENTAL PROTECTION AGENCY
OFFICE OF RESEARCH AND DEVELOPMENT
ENVIRONMENTAL SCIENCES RESEARCH LABORATORY
RESEARCH TRIANGLE PARK, NC 27711

ia

DISCLAIMER

This report has been reviewed by the Environmental Sciences Research Laboratory, U.S. Environmental Protection Agency, and approved for publication. Approval does not signify that the contents necessarily reflect the views and policies of the U.S. Environmental Protection Agency, nor does mention of trade names or commercial products constitute endorsement or recommendation for use.

ABSTRACT

Dry removal of air pollutants from fossil fuel plants is considered both from a modeling and measurement viewpoint. Literature on dry deposition rates is summarized. The processes involved in dry deposition are discussed. The need for the removal rates of specific pollutants is identified; this report considers SO_2, O_3, NO_x, and NO, as well as the total sulfur and lead content of airborne particles.

A prototype field data acquisition system based on a combination of flux gradient relationships was developed, assembled, and tested. The results of the field tests are described.

Significant progress was made in developing the aerosol dry deposition measurement system. Analysis of the sulfur and lead content of aerosols on the filters achieved the required level of relative accuracy for application of the method. Flow rate inaccuracy precluded deposition rate computation.

The vertical profiles of the gases were reasonably linear when considered as a function of the logarithm of height and were consistent with the assumption of dry removal occurring at the surface. A deposition velocity and its experimental accuracy are computed for each field test of gaseous pollutants. These results show generally wide ranges of deposition velocities. The capability of the method to predict the removal rates in certain cases, and its inability in certain other cases is demonstrated.

Recommendations are made for improvement of the capability of the field data acquisition systems and for future applications.

CONTENTS

ABSTRACT iii

LIST OF FIGURES. vi

LIST OF TABLES vii

ACKNOWLEDGMENTS. ix

SECTIONS

I. CONCLUSIONS 1

II. RECOMMENDATIONS 3

III. INTRODUCTION. 5

IV. DRY DEPOSITION MODELS 7

V. EXPERIMENT DESIGN 33

VI. INSTRUMENTATION 44

VII. DATA COLLECTION 60

VIII. RESULTS 65

IX. DISCUSSION. 89

X. REFERENCES. 94

XI. NOMENCLATURE. 104

XII. APPENDICES. 106

FIGURES

Number Page

1. Schematic of Pollutant Concentration Profiles Downwind of a Stack. 34

2. View of Instrumented Tower and Mobile Van with Cooling Tower Plume in Background. 45

3. Nuclepore Filter Mounted on Tower. 46

4. Gas Sampling Systems 49

5. Schematic of Instrumentation Location. 57

6. Diagram of Fetch Around Site. Distances are not to Scale 61

TABLES

Number Page

1. Summary of Deposition Velocities in Literature for Various Gases and Particles. 13

2. Normalized Wind and Pollutant Profiles (Based on Data in References 8, 66). 26

3. Summary of Field Tests During March 1975 at Centralia. 62

4. Total and Normalized Sulfur Aerosol Concentrations Uncorrected for Flow Rate. 67

5. Summary of Computed Aerosol Air Concentrations . . . 68

6. Flow Rate Adjustment (m^3s^{-1}) 69

7. Summary of SO_2 Data Results. 70

8. Least Squares to SO_2 Data. 70

9. Summary of NO_x Profile Results 72

10. Summary of NO Profile Results. 73

11. Summary of Variation Noted in NO_x Profile Data at 0909-0948 73

12. Ozone Profile Summary. 74

13. Least Squares Fit to Ozone Data. 75

14. Summary of Meteorological Data for SO_2 Runs 1-3. . . 76

15. Summary of Meteorological Data for NO_x Runs 1-3. . . 77

16. Summary of Meteorological Data for NO_x Runs 4-6. . . 78

17. Summary of Meteorological Data for NO Runs 1-3 . . . 79

18. Summary of Meteorological Data for O_3 Runs 1-3 . . . 80

19. Summary of Meteorological Data for O_3 Runs 4-6 . . . 81

20. Computed Eddy Diffusivities for Momentum K_m and and Sensible Heat K_h 83

TABLES (continued)

Number Page

21. Deposition Computation for SO_2. 84

22. Deposition Computation for NO_x. 85

23. Deposition Computation for NO 86

24. Deposition Computation for O_3 87

ACKNOWLEDGMENTS

The authors are grateful to Rose Morrill for use of her pasture in Centralia for a test site.

The authors wish to thank Dr. J. M. Hales who made many useful contributions to the progress of the current study. Other Battelle personnel who contributed significantly to the project are Dick Lee, Darrell Joseph, and Rodger Woodruff.

SECTION I

CONCLUSIONS

The surface layer profile method has been shown in these initial tests to have the capability of estimating dry removal rates of pollutants under actual field conditions.

Careful analysis of the experimental accuracy of the computed deposition parameters is a valuable tool for identification of the relative reliance of individual field tests. This technique clearly demonstrates strengths and limitations of the system under initial field tests.

The aerosol test restuls are encouraging. Independent analysis of the sulfur aerosol on the filters demonstrates that the 1 to 2% relative accuracy in concentration needed for dry deposition computation has been achieved. This is a significant breakthrough; it implies that by upgrading the flow rate determination it will be feasible to compute dry removal rates for sulfur-bearing aerosols.

The significant gaseous pollutant profiles indicate dry deposition in a consistent fashion. This is an indication but not proof that the profile accuracies are sufficient for resolution of dry removal rates.

The gaseous pollutant test results clearly demonstrate the importance of considering the specific sources of experimental error. The computation was found to be limited by either or both the pollutant gradient and eddy diffusivity accuracy. The pollutant dry removal rates are expressed as a range of deposition velocities. The resolution was satisfactory only in a few cases.

Sulfur dioxide was computed to deposit at a rate comparable to values in the literature. The results indicate that NO also deposits at a comparable or lower rate than SO_2 but the range is too great to support a definitive conclusion for NO.

SECTION II

RECOMMENDATIONS

Application of the surface layer profile method shows promise of providing considerable information on removal rates of common pollutants, and the relative importance of various processes controlling dry deposition. Modeling efforts should be aimed at developing methods of treating the interaction of these variously limiting processes.

The consistency of the pollutant and micrometeorological profiles was encouraging in the current proof tests of the system. The expansion of the surface layer pollutant profile data base in future experiments should provide a clear indication of the applicability of this approach to determination of dry deposition rates.

Several experiment design modifications are possible to maximize the efficiency of the field effort. First, the use of multiple sites is recommended for future studies. The use of a single tower site is inefficient as a result of extended down times during unfavorable conditions. The efficiency is better as a result of optimum use of field time by sequential use of the sites as dictated by prevailing conditions such as winds, turbulence and pollutant sources. Also in this way a number of combinations of surfaces, conditions, and pollutants can be studied in a single field effort.

Second, it is recommended that turbulence parameterization methods be investigated to calibrate each site. The apparent need to consider each site for meteorological flux computations was discussed recently by Thom, et al[1]. Data sets should be extensive enough to derive a site dependent parameterization of turbulence. This formulation can be used where inherent inaccuracy of the turbulence computation alone limits the removal rate determination.

The overall performance of this method may be improved by specific changes in the detail of the instrumentation systems. Further development in the determination of flow rate in the aerosol sampling system is necessary. Calibrated orifices should be used to reduce the variations in flow rates between levels. Inclusion of inline temperature and pressure measurements at the flow meters is also needed to insure sufficiently accurate determination of the flow rates.

The number of SO_2 samples at each level should be increased to provide better profile accuracy. Multiple monitors should be incorporated into the system for simultaneous sequencing between measurement heights.

For future studies of ozone or other highly reactive gases a roving profiler system with a single line input is recommended to minimize measurement problems.

Further effort is necessary to determine fluxes on the accuracy of the NO_x profiles obtained by the fixed level sequencing method. If this method is not acceptable, then the roving profiler system is considered the best alternative. NO is also a highly reactive gas and a roving profiler system is recommended.

The overall objective in future research efforts should be to develop a semi-empirical relationship for the dry removal of each pollutant. This should be potentially a function of the pollutant, receptor, meteorological variables, and in certain cases the concentration of other pollutants.

SECTION III

INTRODUCTION

Concern with the fate of atmospheric pollutants has intensified interest in removal processes. Transport and diffusion alone have been found insufficient to model ambient pollutant concentrations. Quantitative removal estimates are needed to determine pollutant budgets on large scales as well as to assess local impact from single sources. Possible removal mechanisms include the very slow escape to space from the atmosphere; precipitation and cloud scavenging; chemical transformations; and dry deposition. The current analysis is concerned with the dry deposition processes, emphasizing pollutants in the atmospheric plume from a fossil fuel electrical power station. Both gases and aerosols are considered.

Dry deposition is the direct transfer of a material from the atmosphere to the "earth's surface". Pollutants deposit on soil or vegetation or any other material which comprises the surface of the earth. The adjective dry serves only to exclude transfer by liquid water droplets. No condition is placed on the relative dryness or wetness of the surfaces; dry deposition occurs on deserts as well as oceans.

Dry deposition reduces ambient air pollutant concentrations and determines the potential for an increase in the pollutant concentration on or within the receptor. Processes affecting dry deposition of a specific pollutant include gravitational settling, transport by atmospheric turbulence, impaction, concurrent surface fluxes, and chemical reactions. The quantification of these processes is necessary to evaluate potential pollutant impacts both in the air and on the receptors. This information is needed to develop emission control strategy.

The objective of this program is to develop a comprehensive model which evaluates dry deposition from specific pollutant plumes. The model development requires both theoretical and empirical input. Information based on field studies of the dry deposition of pollutants is relatively scarce. The following section defines the type of information needed to further develop dry deposition models. Subsequent sections describe the development and use of instrumentation, and the field effort which have provided input to the model.

SECTION IV

DRY DEPOSITION MODELS

The earliest understood aspect of dry deposition was gravitational settling of large particles. Early estimates of dry deposition downwind of a stack were based primarily on gravitational settling velocities. However, particles smaller in diameter were predicted to have extremely low deposition rates contrary to experimental evidence. Consequently models were developed which included the effect of atmospheric turbulence on the deposition of intermediate-size particles, for which both gravitation and turbulence are important. Smaller particles still deposited at rates faster than predicted. Molecular transport processes were used to account for these higher rates.

Gravitational models are sufficient for large particles. For particles of an intermediate size gravitational settling can often be important. For example Aylor[2] found that in the low turbulence region within and under vegetation canopies the deposition rate of pollens equals the gravitational settling rate. However, the current study will be limited to particles whose settling velocities are small compared to typical atmospheric eddy velocities. For these smaller particles gravitational settling will not be significant and the gravitational term will be included only as a parallel lower limit for dry deposition.

For gases, gravitational settling rates in the troposphere are unimportant for the normal magnitude of pollutant concentrations.

The modeling of dry deposition in pollutant transport has been incorporated into a number of recent efforts. Examples of these efforts are given in references [3-6]. The methods of modeling will be considered later in this section.

Modeling of the dry deposition of smaller particles and gases has been limited by a lack of data defining the relative importance of various processes. The following model description provides a conceptual framework, which organizes these processes for subsequent study based on the synthesis of a number of references[7-14].

The dry deposition of a substance may be a function of many processes, or one process may dominate all the others. A typical list of interrelated factors includes:

Atmospheric:	Wind speed, turbulence, temperature structure, moisture, pollutant concentration, concentration of other pollutants, solar radiation and long wave radiation.
Receptor:	Surface roughness, moisture, physical and chemical nature, physiological state, membranes, internal and surface pollutant concentration, and status of stomata.
Pollutant:	Chemical and physical properties; solubility, density, size, shape, settling velocity.

Dry deposition involves flux by many different transport mechanisms. These include gravitational settling; atmospheric eddy transport; and molecular transport in the air near the surfaces and from the surface into the receptor. These mechanisms may be grouped into regimes where various processes dominate the transport. These are 1) the atmospheric regime, 2) the surface air layer regime, and 3) the surface into the receptor regime.

The atmospheric regime refers to the air layer over the surfaces, in which the pollutant transport is primarily by eddy motions of air. The surface air layer regime refers to the thin air layer immediately over the receptor, where molecular transport is important. The surface into the receptor regime refers to the rate at which pollutants are transported into the receptor.

The change of a pollutant to another species is a sink that may be a parallel process in any of the regimes. Chemical reactions within the atmospheric regime are not normally rapid enough to be significant when considering the constant flux layer. Reactions at the surface (such as destruction of ozone) and within the surface (such as physiological uptake of SO_2)[15] can be limiting in some situations. Not included in this scheme are components representing potential saturation of various sinks. For example, the deposition to a plant may be a function of the concentrations within the plant. For simplicity such factors are not included in the mathematical model since their inclusion would require retention of time as a variable in the analysis.

Each regime is assigned a resistance (r) which defines the extent to which that regime limits the deposition rate. For a given situation:

$$\frac{1}{r_T} = \frac{1}{r_a + r_\ell + r_i} + \frac{1}{r_g} , \qquad (1)$$

where the subscripts T, a, ℓ, i and g refer to total, atmospheric, surface air layer, internal (surface into receptor), and gravitational resistances respectively. Once total resistance is defined, boundary condition inputs into diffusion models are possible.

Resistance Terms

Each of the resistance terms on the right of Equation 1 will be considered separately below.

Atmospheric Resistance. The processes occurring in the atmospheric regime can be described if the transfer processes for momentum and mass are assumed to be identical. The atmospheric resistance to mass transfer may be assumed to equal that of momentum (τ),

$$r_a = r_\tau = \frac{u(z)}{U_*^{2}} \; . \; . \; . \; . \qquad (2)$$

where u(z) is the wind speed at height z and u_* is the friction velocity. This is the reciprocal of a relationship developed by Chamberlain[15-19] for a "deposition velocity".

The equation for momentum resistance has been proposed to apply to all fluxes to surfaces. However, mechanisms of transport at the surface for momentum and mass differ. Momentum is transferred by pressure forces on the receptor, while mass must be carried to the surface by gravity, impaction, or molecular transport mechanisms. Equation 2 gives the total resistance to momentum flux.

Surface Resistance. The dependence of deposition on near-surface mechanisms comprises the surface resistance term, r_ℓ. Owen and Thompson[3] defined this resistance, arising from molecular interaction in the layer just over the surface, in terms of a nondimensional Stanton number (B^{-1}).

Internal Resistance. For plant tissue, resistance will be a more complicated function of the plant properties and processes. Factors such as membrane pressures and pollutant concentrations may limit transport. The opening and closing of stomata is important for gases. The control of the stomata openings for certain plants has been shown to depend in a complicated fashion on the ambient air concentration of CO_2, H_2O and SO_2. Hence, the resistance in plants appears to be the most difficult resistance to assess, since the properties of the receptor must be defined.

Rates of Reaction Resistances. The limiting processes may be different for gases such as ozone which are highly reactive. Destruction of the gas will occur not only at the surfaces but also in areas shaded by the surfaces. This amounts to a reduced resistance with some material being lost directly from the free atmosphere.

Gravitational Resistance. The gravitational resistance term (r_g) gives a lower limit for the rate of deposition. The resistance is the inverse of the appropriate settling velocity V_s,

$$r_g = \frac{1}{V_s} \quad . \qquad (3)$$

Effective Surface Resistance. An effective surface resistance, r_s, is to be used to include the processes other than atmospheric and gravitational. Assuming the gravitational resistance is large enough to ignore,

$$\frac{1}{r_T} = \frac{1}{r_a + r_s} \quad \ldots \qquad (4)$$

Hence, for computational purposes the effective surface resistance is assumed to be the incremental resistance over the atmospheric resistance to account for the total resistance.

Deposition Velocity.

The simplest expression for dry deposition of either gases or aerosols is based on an assumption relating the ambient air concentrations (χ) and the flux through a surface at a given height (G). At the surface this is the rate of deposition, which is assumed to be directly proportional to the ambient air concentration at a defined height over the surface (z). The constant of proportionality has the units of length per time and is referred to as a "deposition velocity", $(V_d)^{16}$. The equation is:

$$G = V_d/\chi_z \tag{5}$$

with the height traditionally assumed to be 1 meter. This assumes the constant flux layer is one meter deep.

The aim of the modeling effort is to relate dry deposition to processes that are rate limiting. For this purpose the resistance regime concept is preferable to the deposition velocity concept. However, the deposition velocity has been a framework for much of the research in dry deposition, and will be used for summarizing these previous efforts. The deposition velocity through all regimes is the inverse of the total resistance;

$$V_d = \frac{1}{r_T} \quad . \tag{6}$$

Table 1 summarizes deposition velocity estimates for gases and particles to be discussed in the subsequent text. These values are applicable as inverse resistances to the regimes whose effects were included in their determination. For example, values obtained in wind tunnels or static chambers may only partially include the first regime resistances or not. Values derived from atmospheric turbulence alone will apply only to the atmospheric eddy transport regime.

Table 1a. SUMMARY OF DEPOSITION VELOCITIES IN LITERATURE FOR VARIOUS GASES AND PARTICLES.

Substance	Form	Deposition Velocity (cm/sec)	Type of Surface (number of experiments)	Methodology Comments	Reference
Iodine	Gas*	Range: 1.1 - 3.7 Mean: 2.1	Grass (7)	V_d relative to 1m height	Chamberlain[16,19]
Iodine	Gas*	Range: 0.3 - 1.3 Mean: 0.75	Clover Leaves (4)		
Iodine	Gas*	Range: 0.6 - 2.0 Mean: 1.3	Paper Leaves (4)		
Iodine	Gas*	Range: 0.3 - 0.9 Mean: 0.62	Filter Paper (5)		
Iodine	Gas*	Range: 0.09 - 2.43 Mean: 0.87	Grass (19)		Cert Tests[21-26]
Iodine	Gas*	Range: 0.6 - 0.7 Mean: .65	Carbon (12)		

---

*There is some question relative to how long Iodine remains a gas before becoming attached to particles.

Table 1b. SUMMARY OF DEPOSITION VELOCITIES IN LITERATURE FOR VARIOUS GASES AND PARTICLES.

Substance	Form	Deposition Velocity (cm/sec)	Type of Surface (number of experiments)	Methodology Comments	Reference
SO_2	Gas	2.8	alfafa canopy in chambers	Wind speed: 1.8 to 2.2 m/s	Hill (1971)[8]
SO_2	Gas	1.0 - 2.06 Mean: 1.3	Grass (14)	Surface flux determination for SO_2	Garland, et al[27]
$^{35}SO_2$	Gas	0.5 - 2.6 Mean: 1.3	Grass (3)	Radioactivity labeled SO_2 release used as tracer in field experiments.	Owers and Powell[28] *
$^{35}SO_2$	Gas	0.5	Water (1)	Radioactivity labeled SO_2 release used as tracer in field experiments.	Owers and Powell[28] *
SO_2	Gas	0.27 - 1.5 Mean: 0.76	Grass (5)		Shepherd[29] *

---

*Estimates of surface resistance are also given in the paper.

Table 1b. (continued)

Substance	Form	Deposition Velocity (cm/sec)	Type of Surface (number of experiments)	Methodology Comments	Reference
SO_2	Gas	1.8	Short Grass	Surface flux (radioactive tracer)	Garland (1974)[9] *
"		(0.84) 1.3	Medium Grass		
"		0.91	Bare Calcareous Soil		
"		2.2	Fresh water (ph = 8)		
"		<0.50	Forest Pine		
SO_2	Gas	2.4	Over Grass	Lapse	Whelpdale and Shaw[30a]
		2.6		Neutral	
		0.5		Stable	
		1.6	Snow	Lapse	
		0.52		Neutral	
		0.05		Stable	
		4.0	Water	Lapse	
		2.2		Neutral	
		0.16		Stable	

---

*Estimates of surface resistance are also given in the paper.

Table 1c. SUMMARY OF DEPOSITION VELOCITIES IN LITERATURE FOR VARIOUS GASES AND PARTICLES.

Substance	Form	Deposition Velocity (cm/sec)	Type of Surface (number of experiments)	Methodology Comments	Reference
NO	Gas	0	All surfaces	Not a field result	Robinson and Robbins[30b,31]
NO	Gas	0.1	alfalfa canopy	In special chambers	Hill[8]
NO_x	Gas	0.5	alfalfa & oats	derived from data in Tingey[32]	Rassmussen et al[13]
NO_2	Gas	2.0	alfalfa canopy	Special chamber	Hill[8]
HF	Gas	1.6	alfalfa	Fumigation with constant concentrations	Israel[33]
		3.1	field crops	Fumigation with constant concentrations	

Table 1d. SUMMARY OF DEPOSITION VELOCITIES IN LITERATURE FOR VARIOUS GASES AND PARTICLES.

Substance	Form	Deposition Velocity (cm/sec)	Type of Surface (number of experiments)	Methodology Comments	Reference
O_3	Gas	0.7 - 1.7 Mean: 1.13	Several	Review of research by several authors[34-39]	Galbally[39]
O_3	Gas	0.6 - 1.8	Soil, peat, grass	Wind tunnel experiments	Garland (1974)[9]
O_3	Gas	1.4 - 6.3	Several	Decay rate experiment in box	Garland (1974)[9]
O_3	Gas	1.7	Alfalfa canopy	Special chambers	Hill[8]

Table 1e. SUMMARY OF DEPOSITION VELOCITIES IN LITERATURE FOR VARIOUS GASES AND PARTICLES.

Substance	Form	Deposition Velocity (cm/sec)	Type of Surface (number of experiments)	Methodology Comments	Reference
Fission Products	Particle	0.07	Gummed paper	Surface activity measurements particles are formed by an electric core.	Megaw and Chadwick[40]
^{137}Cs	Particle	0.9	Water (5)	Field release test measurements.	Convair[41-43]
		0.04	Soil (15)		
		0.2	Grass (21)		
		0.2	Sticky paper (117)		
^{103}Ru	Particle	2.3	Water (9)		
		0.4	Soil (16)		
		0.6	Grass (20)		
		0.4	Sticky paper (8)		
^{93}Zr, ^{95}Nb	Particle	5.7	Water (6)		
		2.9	Soil (6)		
		1.4	Sticky paper (10)		

Table 1e. (continued)

Substance	Form	Deposition Velocity (cm/sec)	Type of Surface (number of experiments)	Methodology Comments	Reference
$^{141}\mathrm{Ca}$	Particle	0.7	Sticky paper		Convair[41-43]
$^{127}\mathrm{Te}$', $^{129}\mathrm{Te}$	Particle	0.7	Sticky paper (8)		
Pb	Particle	0.13	Dilute HCl solution	Plastic pluviometer	Servant[44]
Trace Elements	Particles	.04 to 0.3	Deposition plates	Industrial substances	Cawse & Peirson[45]
Trace Elements	Particles	0.3 to 1.0	Deposition plates	Soil-derived substance	
Zinc Sulfide	Particles (diameter of 2.5μm)	0.5	Sage brush	Stable atmospheric conditions.	Simpson[46]
Particles of 0.1μm		0.2 - 9.2	Desert		Islitzer & Dumbauld[47]
Natural Particulate Material		0.8 - 7.6 (7)	Great Lakes (water)		Whelpdale[48]

Several recent reports have reviewed the dry deposition processes for common pollutants[13,14,49]. The reader is referred to these for additional information. References 13 and 14 include discussion of chemical reactions that appear to be controlling the deposition rates.

Although the emphasis in this review is on certain fossil fuel pollutants, other substances have been included to demonstrate the general range of deposition velocity values. Dry deposition of radioactive substances comprises a large part of the available information.

Particles

Reported values of dry deposition of particles from the atmosphere also shows a wide variation. In England, deposition studies of atmospheric trace elements onto artificial surfaces produced deposition velocities which varied from less than 0.04 cm/s to 0.3 cm/s for apparently industrial substances, and 0.3 to about 1.0 for soil-derived substances[45].

The deposition of small fluorescent particles was studied by Simpson[46] at Hanford, and Islitzer and Dumbauld[47] at the National Reactor Testing Station. Simpson's data for near ground release of zinc sulfide particles (mean diameter 2.5 μm) under stable conditions were used by Islitzer and Dumbauld to calculate an average deposition value of 0.5 cm/s. Islitzer and Dumbauld, using particles of 1 μm, obtained deposition velocities that ranged between 0.2 and 9.2 cm/s, with a mean value for all experiments of 4.6 cm/s. Inversion conditions consistently had the lowest values (0.2 cm/s) which were comparable to Simpson's results. Deposition velocities of 2.4 and 7.1 cm/s were computed for the neutral and lapse conditions respectively.

Table 1 includes results of U. S. Air Force studies of radionuclide deposition[41,42]. The properties of these radionuclides are not clearly defined; as a result, they cannot be readily applied to deposition of other substances. However, they do indicate a wide range of possible values.

In a review paper, Gifford and Pack[50] conclude that the average deposition velocities for radioactive materials (^{131}I, SO_2, Ru) are less than 1 cm/sec on flat plates or bare soil, and between 1 and 3 cm/sec on vegetation. For inert material he gave values of less than 0.1 and 0.1 to 0.2 cm/sec for deposition on flat plates or bare soil and vegetation, respectively.

A study by Megaw and Chadwick[40] of the deposition of fission products using surface activity measurements yielded deposition velocity values ranging from 0.07 cm/sec on gummed paper to 0.2 cm/sec on grass. These fission products were submicron particles produced by an electrical arc.

In a recent paper, Nickola and Clark[51] reported about 7% of a ZnS particle plume deposited within 842 m downwind of release, in a moderately stable atmosphere. For two other runs under very stable and unstable conditions, 1% or less deposited within distances of 812 and 200 m respectively. Estimates of deposition velocities were not made in this paper, although these dual tracer results suggest that some earlier studies may overestimate deposition rates.

Although there is considerable information on the rate of fallout of particles from upper atmospheric sources, the fact that washout has been identified as a major mechanism for removal precludes the use of this data except where wet and dry removal can be separated. For example, a study of fallout materials where dry and wet were separated at Kjeller gave average annual dry deposition velocities in 1957 and 1958 of 0.51 and 0.75

cm/sec. Individual average monthly values ranged between 3.4 and 0.2 cm/sec[52].

The point of emission of a particle in the atmosphere can influence the importance of certain removal processes. Marenco and Fontan[53] demonstrate by numerical models that a particle produced at ground level will be eliminated chiefly by dry deposition, whereas a particle produced near the tropopause will be removed primarily by rainout. These authors also point out that the residence time differs for particles produced near the ground or near the tropopause because of the change in process importance.

The surface and receptor resistances of particles have been studied in wind tunnels. Sehmel[54-57] has considered the effects of variations in wind speed, particles sizes and surfaces; and shows that deposition velocities change significantly with wind speed and particle size. For 0.3 μm particles, (ρ = 1.5 g/cm^3), the wind tunnel deposition velocity on a simulated grass surface was .08 cm/s for a 5 mph wind and about 0.2 cm/s for a 30 mph wind. A field experiment using the same surface and 0.7 μm mean diameter rhodamine particles gave a total deposition velocity of 0.2 cm/s which compared well with a total deposition velocity of 0.17 cm/s extrapolated from the wind tunnel data for this size particle. In the wind tunnel studies, the deposition velocities were found to be a function of particle size. The minimum deposition velocities were fairly constant within the range 0.1 to 1 μm particle diameters. Particles larger or smaller than this deposited more rapidly. The effect of a change in surface roughness was studied using two sizes of crushed gravel. For 0.3 μm diameter particles and a wind speed of 5 mph, the deposition velocities were measured on gravel between 1.6 cm and 3.8 cm diameter. The deposition velocities varied from 0.01 cm/s to 0.04 cm/s respectively.

Sehmel[56,57] has developed a model based on wind tunnel data. When deposition velocity is considered as a function of particle size, a minimum value is found in the relationship. His results indicate that this minimum deposition velocity increases rapidly as both wind speed and surface roughness increase; it is a minor function of atmospheric stability. The model can be used to predict deposition velocities (for a natural roughness height of 3 cm) of about 0.20 cm/s for 1 m/sec winds and 3.3 cm/s for 7 m/sec winds.

Hicks has proposed a model for deposition velocity of rapidly depositing gases based on the mean wind speed at a fixed height[58].

Gases

The resistance can be expected to be the same for all gases in the atmospheric transport regime. The resistances in the layer over and on plant surfaces are functions of the molecular transport processes over the surface and the potential for the uptake of gas on or within the surfaces. Hence, surface resistances of each gas must be considered separately.

The uptake of noble gases by natural surface will be very slow. Therefore, resistance in the third regime is very high, and significant deposition does not occur.

A comprehensive survey of the sources and natural removal processes for atmospheric gaseous pollutants (including sulfur, carbon oxidants and organic-containing gases) has been compiled[13]. This survey contains considerable information on the gases considered in this report, as well as on ammonia and carbon monoxide.

Gases such as SO_2 and iodine, which are absorbed on most natural surfaces, have a low surface regime resistance. Studies show that deposition of iodine often occurs at a rate primarily controlled by atmospheric turbulence[6,16,19,21-26]. This implies the surface is nearly a perfect sink.

Because of its relatively rapid absorption onto surfaces, it is not certain whether iodine should be considered a gas or a particle. The release may be a gas but it is uncertain how fast the iodine will attach to particles in the atmosphere. The deposition velocity and the biological half-life of elemental iodine on grass and foliage have been the subject of recent investigations at the Julich Research Center in Germany[59]. Results indicate the deposition velocity (or inverse of total resistance) is a function of biological and meteorological variables. A semi-empirical relationship was developed which includes the dry weight of vegetation per unit area, the friction velocity, the relative humidity and a biological factor.

Studies of SO_2 deposition show that either the atmospheric or surface regimes can be limiting. The state of stomata openings, surface radiant energy budget, and the wetness of the surfaces are surface properties that may control resistance in the surface regime. Information on the actual concentrations of SO_2 in plants is contained in a study by Pyatt[60]. Martin and Barber[61] documented the loss of SO_2 near a hedge. Mansfield and Heaten[62] studied the changes in stomatal openings at low SO_2 concentrations in _Xanthium_.

Spedding[63] studied the effects of relative humidity and stomata conditions for the uptake of SO_2 on barley. He found a considerable range of resistance to uptake. These results may be particularly useful in modeling efforts since they are summarized in terms of deposition based on plant surface area. Spedding[63] confirmed that stomatal intake at high humidities and absorption on thin water films can both be significant in the rate of SO_2 uptake. His measurements were based on experiments with radioactively labeled SO_2. Majernik and Mansfield[64] state that even though conditions are sufficient for SO_2 to stimulate stomatal opening, the presence of sufficient CO_2 can result in stomatal closing. This indicates that the removal rate of SO_2 may be a function of concurrent CO_2 concentration over a plant layer.

Relative rates of uptake of various pollutants in the soil are factors in the surface resistance term. Abeles, et al.[65] present data supporting the hypothesis that microbial or chemical reaction rates of ethylene, other hydrocarbons, SO_2, and NO_2 are sufficient for dry removal to be a significant sink. Ethylene uptake was not found with sterile soil or in soil lacking oxygen. Significant uptake did occur with ethylene in air over soil. The decay time for ethylene in air was such that uptake was nearly complete in four days, indicating that microbial reactions are important. For SO_2 and NO_2 the rates were faster. In 15 minutes SO_2 was reduced from 100 ppm to 8 and 20 ppm for soil and autoclaved soil, respectively. Nitrogen dioxide reduced from 0.100 ppm to 3 and 13 ppm after 24 hours for soil and autoclaved soil. These results suggest that chemical reaction is dominant, although some allowance should be made for microbial reactions.

The absorption and resultant profiles of gaseous air pollutants by alfalfa canopies were studied in an environmental growth chamber[8,66]. Hydrogen fluoride, SO_2 and NO_2 profiles suggested efficient removal by both the upper and intermediate surface vegetation. Interpolation of their profile data suggests that none of the gases were transferred to the canopy as efficiently as momentum. Table 2 has been derived from their data to show the efficiency of transfer of momentum and gases as a function of height. Their data has been normalized to the top height to allow comparison of the shape of the profiles. Assuming the transport mechanisms are the same for all properties within the

Table 2. NORMALIZED WIND AND POLLUTANT PROFILES (BASED ON DATA IN REFERENCES 8,66)

Height (cm)	% Momentum*	% SO_2	% O_2	% HF	% NO_2	% NO
60	100%	100	100	100	100	100
50	91	92	94	94	96	98
40 (canopy)	37	69	74	75	90	100
30	13	47	54	59	75	93
20	8	37	42	53	62	92
10	5	22	36	51	57	94
Changes						
60-50	9	8	6	6	4	2
50-40	54	23	20	19	6	-2
40-30	24	22	20	16	15	7
30-20	5	10	12	6	13	1
20-10	3	15	6	2	5	-2

*(Value at height/Value at 60 cm) x 100

air, the profiles may be interpreted as reflecting fluxes. These profiles indicate that momentum transfer is more efficient than any of the pollutants. Use of momentum deposition velocities will overestimate the flux and the location of the deposition. Although significant deposition of the gases (except NO) occurs, the deposition is clearly occurring deeper into the canopy than is the momentum transfer as indicated by the changes in concentration with height. Alfalfa canopies removed gaseous pollutants in the following order: hydrogen fluoride > sulfur dioxide > chlorine > nitrogen dioxide > ozone > peroxyacetyl nitrate > nitric oxide > carbon monoxide. These results show the variation in deposition rates for different gases.

The exchange over water surfaces was considered from a phase-resistance view by Liss[67], who tentatively concluded that the vertical gradients of SO_2 and water vapor close to the sea surface should be similar, and the mean residence time of SO_2 and a water vapor molecule should be of the same order (10 days). He compared the resistances in the liquid and gas phases and found the gas phase to be limiting at a pH greater than about 2.8. He noted that this transition pH could vary from 2.5 to 4 for the variation between calm and turbulent conditions (in both phases). In a more recent paper, Liss and Slater[68] consider the relative resistances in gas and liquid phases for SO, N_2O, CO, CH_4, CCl_4, CCl_3F, MeI, $(Me)_2S$. For all except SO_2 the surface resistance was dominated by the liquid phase. Estimates of exchange coefficients are given based on available literature data.

Flux determinations of SO_2 deposition rates over specific surfaces has been the topic of several recent papers. Garland et al.[27] used surface layer flux techniques to study the deposition rates of SO_2. They computed the relative atmospheric and "surface" resistance terms. Garland[9] compared surface layer flux techniques with deposition of a radioactive tracer. Shepard[29] used the surface layer flux technique to study dry deposition over grass and water.

Owens and Powell[28] used the radioactive tracer method to study SO_2 dry deposition over land and water. Their paper presents SO_2 dry deposition rates which are fairly consistent with those summarized in Table 1. References 69-71 provide additional information on SO_2 uptake over water.

The capacity for various soils to take up SO_2 and other pollutants under a variety of conditions has been the topic of several papers. Situations where soil absorption may be dominant will require modeling a soil resistance term. The results of Bohn[98], Payrissat and Beilke[72] (SO_2), Fisher[73] (SO_2), Smith, et al.[74] (SO_2, H_2S, CH_3SH, C_2H_4, C_2H_2 and CO), and Terragilo and Manganelli[75] (SO_2) will be useful in this task for soils.

The vertical flux of O_3 has been considered by a number of authors as given in Table 1. O_3 appears to have a fairly rapid removal rate, suggesting the atmospheric transport will be primarily limiting.

Regener and Aldaz[38] suggest O_3 as an alternate flux measurement to determine atmospheric turbulence when standard techniques for momentum or sensible heat do not apply. Ozone was assumed to be destroyed at the surface, with atmospheric turbulence limiting the rate of transport to the surface and hence determining the flux rate for nocturnal conditions. A destruction coefficient was defined and is taken here to be equivalent to a deposition velocity or inverse resistance.

In a paper which considers the sources and sinks of gaseous nitrogen compound pollutants, Robinson and Robbins[31] state that gaseous deposition of NO is negligible. Gaseous deposition for NO_2 is calculated based on a deposition velocity of 1 cm/sec[31]. This deposition velocity was an approximation from experimental data over alfalfa and oats in Reference 32.

Application of Model

Although primitive, the present deposition model can be used to improve modeling efforts requiring dry deposition estimates. The basic dry deposition values (deposition velocities or resistance values) are chosen from the literature and vary as physical processes dictate. The deposition of SO_2 will be used as an example of a reactive gas that deposits rapidly on surfaces. The literature shows high deposition velocities (low resistances) for SO_2. There is some information on the relative values of the atmospheric and total resistances for SO_2. In a simple model, the total resistance to deposition can be defined as the sum of the surface resistance (a constant estimated from the literature) and the atmospheric resistance. The latter can be varied with wind speed and roughness length using the relationship for atmospheric resistance given in the model section.

Sulfur-bearing particles are generally about 0.2μm in diameter, and are thought to have deposition rates an order of magnitude smaller than SO_2. The order of magnitude higher resistances for sulfur aerosols imply that surface resistance is considerably more limiting for sulfur aerosols than for SO_2. The same approach to estimating deposition can be used, that is summing a surface resistance and atmospheric resistance. The variation in dry deposition of sulfur aerosols because of atmospheric changes will be considerably less, perhaps often negligible because the surface is limiting. In this case, a more detailed surface model is necessary to estimate the surface resistance as a function of ambient conditions. A model accounting for impaction and surface area appears applicable. The current field effort is designed to provide estimates of the variation of total and atmospheric resistances of sulfur aerosols under various field conditions.

Applications in Computational Models

In the gaussian diffusion model the total resistance may be used directly to estimate deposition over a given point based on the air concentration at that point:

$$G = \chi / r_T \quad . \; . \; . \; . \qquad (7)$$

This technique fails to account for progressive depletion of the plume downwind. To the extent that diffusion nomograms can be expected to include deposition effects inherent in the field data on which they are based, this technique is justifiable. Where deposition for extended distances is considered, the model may account for mass loss by deposition by modifying the nomograms as a function of distance. Without this correction it is possible to compute more pollutant removed than there is mass of pollutant. When great distances are considered, the failure of the model to account for mass loss by deposition can cause large errors.

A single point relationship may be used as a boundary condition when a finite difference K theory model is utilized. At each grid point the flux to the surface is given by:

$$G(x,y,z=0) = \chi(x,y,z=0/r_T(x,y,\ldots) \qquad (8)$$

This formulation presents the total resistance as a function of the spatial coordinates of the surface, allowing incorporation of additional variables that research may reveal. These variables can be specific to a gas or particle and may include processes in the various regimes discussed earlier.

When the gaussian model is used for extended distances, the total resistance may be used directly to estimate depletion by a source depletion model. Following the notation of Horst[76] the downwind air concentration including loss by deposition and diffusion is given by:

$$\chi(x,z) = Q\ D\ (x,z,h)\ \exp - \int_0^{\chi} \frac{D(\xi\ z_d,h)}{r_T}\, d\xi \qquad (9)$$

where,

D = diffusion function (sec m^{-2})
χ = crosswind-integrated air concentration (units m^{-2})
Q = source strength (units sec^{-1})
x = downwind distance coordinate (m)
z = height of receptor (m)
h = height of diffusion source (m)
r_T = total resistance
ξ = downwind coordinate of surface source, variable of integration (m)

where D is defined as:

$$D(x,z,h) = \frac{\chi(x,z)}{Q} \quad . \qquad (10)$$

This is not difficult to apply once the total resistance is defined, but it fails to consider that depletion occurs on the surface. With this model the depletion occurs throughout the entire vertical extent of the diffusing cloud.

Horst[76] developed an alternative model which accounts for surface depletion within the framework of a gaussian model. The calculated downwind air concentrations include the effects of resuspension, weathering and deposition as a function of time. Considering the special case for a time independent source and deposition processes only results in the relationship for the depleted and diffused air concentration;

$$\chi(x,z) = Q\ D(x,z,h) - \int_{o}^{\chi} \frac{\chi(\xi,z_d,h)\ D(x-\xi,\ z,\ h = o)}{r_T}\, d\xi \qquad (11)$$

where the symbols are the same as for Equation 9.

Horst made a comparison between the two approaches (Equations 9 and 11) for various initial release heights and stabilities and assuming $\frac{1}{r_T\overline{u}} = 10^{-2}$ where $\overline{u}$ = mean wind speed. The results show that the source depletion model overestimates the surface air concentration by factors of 2 to 4 in some cases. This effect results in the rate of decrease of mass downwind in the surface depletion model being smaller, and hence at large downwind distances the surface depletion model eventually has surface air concentrations that are greater than those of the large depletion model. The cross-over distance where the concentrations (at 1m height) are equal is almost 10 km downwind for very stable conditions. The differences for unstable and neutral conditions are not as great.

Elderkin et al.[77] have modeled deposition processes in terms of the turbulence parameters and compared their model with field results.

SECTION V

EXPERIMENT DESIGN

The objective was to design a field experiment to provide information on the rates of removal of various pollutants. The gases studied were SO_2, O_3, NO_x and NO. The aerosols contained lead and sulfur. The surface layer profile flux determination technique appeared best able to obtain quantitative information on removal rates. The initial experiment design was presented in Reference 29, which was published in the proceedings of Atmosphere-Surface Exchange of Particulate and Gaseous Pollutants.

A primary requirement of this experiment was that the measured profiles be controlled by the local surface fluxes. An ideal conceptualization of the processes influencing the vertical concentration profile of a pollutant downwind of a stack is given in Figure 1. Immediately downwind of the stack is an area where the pollutant does not effectively reach ground level. At greater distances, the deposition rate for smaller particles becomes progressively a function of both the settling velocity and the eddy movements of the particles. Then for particles with settling velocities much smaller than typical eddy velocities of the air, the deposition becomes a function of turbulence and the surface properties.

Gases can be expected to be diffused with these smaller particles. Gaseous pollutants will not normally undergo the gravitational settling phase. Certain conditions could exist that could skew downwind the vertical profile of various gases in any of the phases in Figure 1. Particles or liquid droplets falling through a plume may redistribute gases in the vertical profile, as shown in a study by Hales, et al.[79].

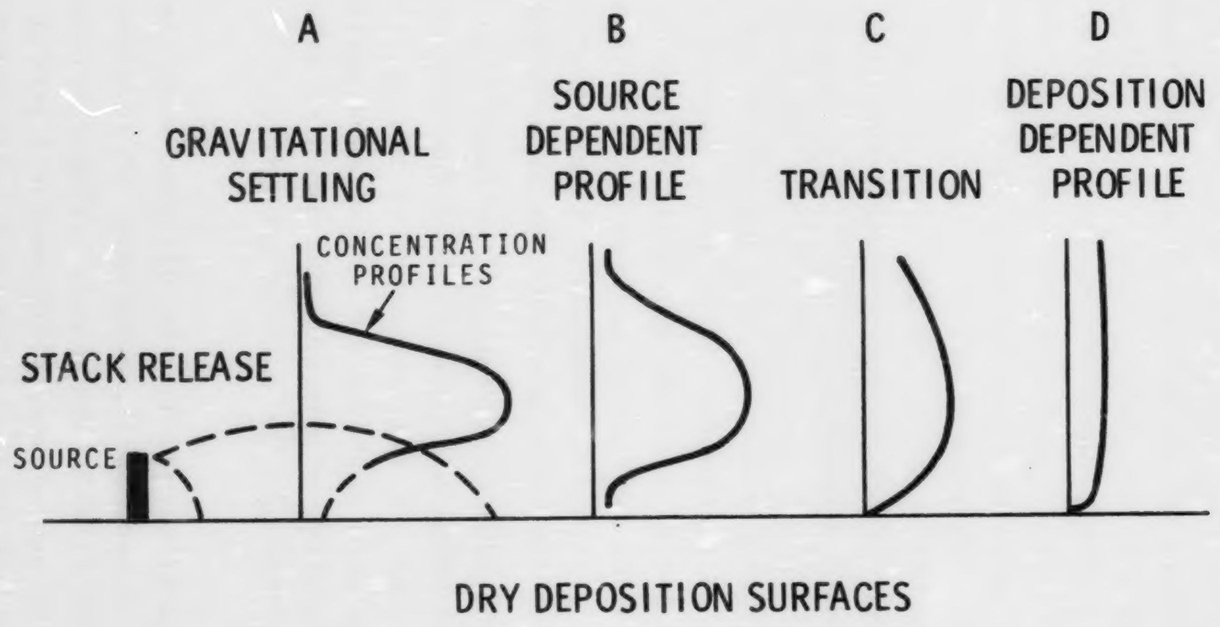
A
B
C
D
GRAVITATIONAL SETTLING
SOURCE DEPENDENT PROFILE
TRANSITION
DEPOSITION DEPENDENT PROFILE
CONCENTRATION PROFILES
STACK RELEASE
SOURCE
DRY DEPOSITION SURFACES

FIGURE 1. SCHEMATIC OF POLLUTANT CONCENTRATION PROFILES DOWNWIND OF A STACK.

For both gases and particles, the source dependent profile is in the region where the vertical profile is still determined by the source configuration. For hot plumes the buoyant characteristics of the plume control the initial dispersion. However, as the plume mixes with ambient air both the pollutants and the excess heat become diluted. The transition stage is where the effects of both source and dry deposition appear in the vertical structure of the air concentration profile. Further downwind the source profile configuration is lost and the vertical profile reflects only the effect of removal by dry deposition.

This is an idealized discussion to illustrate the progression of processes. Diurnal changes and local variations in the atmosphere can greatly influence the processes.

Computational Basis

Dry deposition may be considered as a flux of the pollutant from the air to a receptor. Although in practice this flux may vary with distance from the receptor, horizontal homogeneity is assumed. That is, the average characteristics of the receptors and the atmospheric delivery processes are assumed constant horizontally. This requires a sufficient upwind fetch to allow development of a horizontal equilibrium of the dry deposition processes. Any vertical variation represents the flux of material from various heights to the receptors at ground level. The current effort requires that measurements be in the constant flux layer over the surface where the flux does not change significantly with height.

The vertical flux (G), of the pollutant with air concentration χ may be described in a gradient flux relationship:

$$G = -K \frac{\partial \chi}{\partial z} \qquad (12)$$

where K is the eddy diffusivity for the pollutant. When dry deposition is occurring, the gradient $\frac{\partial \chi}{\partial z}$ would be positive. This results in a flux towards the surface.

Equation (12) is applied to a layer of air over the receptors where eddy flux is the dominant mechanism for transport. Once the flux for the pollutant has been determined, the resistance r_T (inverse deposition velocity) at height z is given:

$$r_T = \chi/G = \frac{\chi_z}{K_z \left(\frac{\partial \chi}{\partial z}\right)_z} \; . \; . \; . \; . \qquad (13)$$

In the constant flux layer over the surface the total resistance appears to be a function of height. Consider the middle expression in Equation 13. The denominator, G, is a constant with height in the constant flux layer, and the numerator, χ_z, will decrease near the surface when dry deposition is occurring. Hence, higher and lower apparent resistances can be computed from the same data set using higher and lower heights to define the air concentration. The exponential nature of the surface layer profiles suggests the effect will be greatest near the surface and decrease with height. The upper level of data acquisition has been adopted for the current study to minimize this effect. Adjustment of results to a standard 1m level will be a function of prevailing micrometeorological conditions.

Equation 13 defines the total resistance for the flux of material to the surface. The effects of all regimes are included. The atmospheric pollutant gradient reflects the combined effects of atmospheric turbulence and rates of removal near or on the environmental surfaces. The total resistance equals the atmospheric resistance only when all other resistances are sufficiently small.

The application of Equation 13 requires defining diffusivity K. In finite difference form Equation 13 becomes:

$$\frac{1}{V_d} = r_T = \frac{\chi_z}{K}\left(\frac{\Delta z}{\Delta \chi}\right) = \frac{1}{K\left(\frac{\Delta\chi/\Delta z}{\chi}\right)} = \frac{\Delta z}{K}\,\frac{(\chi)}{(\Delta\chi)} \qquad (14)$$

where clearly the resistance is a function of the eddy diffusivity and the fractional change of concentrations with height approximated over a finite layer. Direct determination of the eddy diffusivity for pollutant particles or gases is generally not possible. Instead, eddy diffusivities for concurrent fluxes are principally momentum, sensible heat, and latent heat, although literature exists on the possibility of using ozone or radon[39,80].

To determine a particular eddy diffusivity two flux relationships are equated and solved for the eddy diffusivity. The first (Equation 12) is the Fickian relationship between the vertical gradient of the concentration of the material to be transported, $\frac{\partial\chi}{\partial z}$, and the flux of the material, G. The second relationship is the eddy flux equation:

$$G = (\overline{\chi' w'}) \qquad (15)$$

where w is the vertical velocity and primes refer to departures from the mean. The application of these requires definition of terms. For momentum flux, $G = \tau$ and $\chi = \rho\bar{u}$, (τ = momentum flux, ρ = density of air, $\bar{u}$ = mean wind speed); for sensible heat flux $G = H$, and $\chi = \rho Cp\bar{\Theta}$, (H = sensible heat flux, Cp = specific heat at constant pressure for air, Θ = potential temperature); and for latent heat, $G = LE$ and $\chi = \rho Lq$ (E = water vapor flux, L = latent heat of evaporation for water, q = specific humidity). Equating the two flux relationships and substituting definitions of χ, the following relationships for eddy diffusivities may be obtained:

$$K_m = + \frac{(\overline{u'w'})}{\frac{\partial u}{\partial z}} \tag{16}$$

$$K_H = + \frac{\overline{\Theta'w'}}{\frac{\partial \Theta}{\partial z}} \tag{17}$$

and

$$K_q = \frac{(\overline{q'w'})}{\frac{\partial q}{\partial z}} . \tag{18}$$

K_m, K_H and K_q are the eddy diffusivities for momentum, sensible heat and latent heat respectively. The use of and the relationship between these eddy diffusivities are currently under discussion. When any of the vertical gradients are near zero (or below measurement capability) the eddy diffusivity is not defined, and the technique cannot be used. When the flux of the material is zero the eddy diffusivity is also undefined. In addition, there is no requirement that various fluxes are necessarily zero at the same time.

In addition there may be basic differences in the transport for various properties or substances. The sensible heat transport is affected by the inherent tendency for updrafts to be warmer air and downdrafts cooler air, with no corresponding mechanism for momentum flux. Whether a certain similar inherent bias may occur in pollutant fluxes is unknown.

Exact analogies between the various fluxes require that the transport mechanisms be identical. To the extent that these are similar, the corresponding vertical profiles will exhibit similar shapes. The vertical fluxes of sensible heat, latent heat, momentum and a pollutant are reflected in the mean vertical profiles of potential temperature, water vapor, wind speed, and pollutant concentration. An irregular vertical change such as caused by a discontinuity (inversion layer, etc.), will normally be reflected in some manner in each of the profiles. In this way the similarity of the shapes of profiles is useful for excluding cases with obvious vertical flux divergence.

Without detailed study, the choice of the appropriate eddy diffusivity must be qualitative and to a certain extent arbitrary. One convention is assuming that momentum eddy diffusivity is applicable. The additional surface resistance caused by molecular processes on the gas deposition surfaces may be considered using the dimensionless reciprocal Stanton number[81]. This is equivalent to the use of a surface resistance in the current study. The surface resistance should also be applicable to aerosol deposition with different processes producing a surface resistance.

Another convention is assuming that an eddy diffusivity for heat or water vapor is appropriate. A special case is the use of an apparent eddy diffusivity obtained by an energy budget method which assumes the heat and water vapor eddy diffusivities are equal, or that their ratio is known. The surface resistance should apply with use of the heat or moisture eddy diffusivity in a similar fashion.

There is no reason to suspect the source-sink relationships between any of these fluxes and the pollutant flux are identical under all conditions. Results based on either eddy diffusivity should be interpreted as relative fluxes because the estimated value of eddy diffusivity may be in error.

If momentum eddy diffusivity is assumed, then the flux, G, of a pollutant with air concentration χ and corresponding resistance r_T, may be expressed as follows with values defined at level z,

$$G = \left(\frac{(\overline{u'w'})}{\left(\frac{\partial \overline{u}}{\partial z}\right)_z} \left(\frac{\partial \chi}{\partial z}\right)_z \right) \qquad (19)$$

$$\frac{1}{V_d} = r_T = \frac{\chi_z}{(\overline{u'w'})} \frac{\left(\frac{\partial \overline{u}}{\partial z}\right)_z}{\left(\frac{\partial \chi}{\partial z}\right)_z} \qquad (20)$$

This may be written in finite difference form for computation;

$$G = - \left(\frac{(\overline{u'w'})}{\frac{\Delta u}{\Delta z}_z} \right) \left(\frac{\Delta \chi}{\Delta z}\right)_z \qquad (21)$$

$$\frac{1}{V_d} = r_T = \frac{\chi}{(\overline{u'w'})} \frac{\left(\frac{\Delta \overline{u}}{\Delta z}\right)_z}{\left(\frac{\Delta \chi}{\Delta z}\right)_z} \qquad (22)$$

The variables that need to be measured to determine G and r_T are: the horizontal and vertical wind speed (at a sampling rate and with an instrument time response sufficient for eddy flux calculation); the vertical gradient of mean wind speed; the vertical gradient of air pollutant concentrations; and the air pollutant concentration.

Using the alternate heat flux analogy, the air temperature and vertical wind velocity must be measured at a sampling rate and with an instrument time response sufficient to calculate an eddy flux plus a vertical gradient of potential temperature.

The definition of the conditions where the surface flux method is applicable places constraints on the location and sampling periods which can be used. The fetch conditions for development of a surface layer profile of wind and temperature have been defined in experimental studies of momentum and heat transfer. The literature contains estimates based on canopy heights and local roughness elements. Ultimately each site must be considered individually including the prevailing conditions during the experiments. As a general rule, the surface flux approach cannot be applied unless 1) air containing the pollutant moving over a site has been well mixed vertically up to a sufficient depth and 2) the site meets equilibrium surface layer fetch requirements defined by the site characteristics. These are the minimum conditions for application of the flux model at a specific location.

A study of carbon dioxide profiles over a wheat crop showed that the horizontal variation in the concentration difference was small enough that a single tower should be adequate[82]. If the pollutant uptake can be assumed to be as uniform as the CO_2 emissions, then this supports the current design of using a single instrumented tower to determine profiles over representative surfaces.

Experimental Accuracy

The experimental accuracy is estimated by application of the theory of sampling. The experimental error for each mean value is estimated. These are then propagated through the computation of a deposition velocity (inverse total resistance). The accuracy of the pollutant gradient and the eddy diffusivity are also limiting factors in the computation.

The initial estimates of accuracy require judgements of the magnitude and randomness. As a result, the final accuracy estimates are partly arbitrary, but they are a useful measure of the relative accuracy between experiments.

Gradients. Gradients are computed from differences in concentrations divided by differences in heights. The accuracy of the height differences is estimated to be better than 0.3%. As a rule, the accuracy of the pollutant concentrations between measurement heights is estimated to be up to an order of magnitude better than the absolute accuracy. Direct assessment of the relative accuracy is not possible with the current experiment design, although relative accuracy may be indicated by the consistency of the vertical pollutant gradients with concurrent meteorological gradients.

Eddy Diffusivity. The eddy diffusivities are computed for Equations 16 and 17 for momentum and heat respectively. The expression for the experimental error is

Exp. Error =

$$\left[\left(\frac{\overline{aw}}{g}\right)^2\left(\left(\frac{\sigma_a}{a}\right)^2+\left(\frac{\sigma_w}{w}\right)^2\right)+\left(\frac{\sigma_y}{g}\right)^2+\left(\frac{\overline{aw}}{g}\right)^2\left(\left(\frac{\sigma_{\overline{aw}}}{aw}\right)^2+\left(\frac{\sigma_{\overline{g}}}{g}\right)^2\right)\right]^{1/2} \qquad (23)$$

where for heat $a=\Theta$ and $g=\Delta\Theta/\Delta z$, and momentum $a=u$ and $g=\Delta\overline{u}/\Delta z$. The σ's refer to the estimates of the experimental standard deviations for the subscripts. This assumes the errors are random. In practice, the value of $\sigma_{\overline{aw}}$ was assumed to equal ±.05% of $\overline{uw}$ or ±.02% of $\overline{\Theta w}$.

The advantage of this analysis is that it keeps track of the accuracy in automated computations. Note that, the terms $\overline{u'w'}$ and $\overline{\Theta'w'}$ in Equations 16 and 17 are computed from the difference of two terms.

$$\overline{u'w'} = \overline{uw} - \overline{u}\,\overline{w} \qquad (24)$$
$$\overline{\Theta'w'} = \overline{\Theta w} - \overline{\Theta}\,\overline{w}$$

These difference terms can generate an answer which is "noise" when the terms are nearly the same size. Equation 23 combines this and other computations into a single estimate of the accuracy of the K values.

SECTION VI

INSTRUMENTATION

Field Instrumentation

Development and field demonstration of measurement systems applicable to the surface flux measurement concept is the current goal. These systems involved areas of surface layer micrometeorology and air pollution chemistry.

This section will discuss the systems that were designed, assembled and tested. The systems that were chosen for the field testing and demonstration effort will then be described. The basic field system is composed of a tower for placement of filters, sensors, and air intake lines at various heights to obtain vertical profiles of pollutants and meteorological variables. A mobile laboratory is used as a base of operation and contains the analyzers and recorders. The gas and aerosol systems will be considered separately after a discussion of common elements. The micrometeorological measurement system used in conjunction with both the gas and aerosol systems will be discussed in the final section. Photographs of the complete field instrumentation and filters are given in Figures 2 and 3.

Common Components

The air intake lines between the tower and flow meters were 12.7 mm diameter Teflon tubing with stainless steel swage lock fittings. Teflon wedges and collars were used in the Swage lock fittings. Teflon tubing 6.35 mm in diameter was used for all connections from the tower to the mobile laboratory. Stainless steel or all-teflon Swage lock fittings were used. The sampling lines were enclosed in a heated, insulated aluminum casing. The lines can be heated in situations where condensation may be problem.

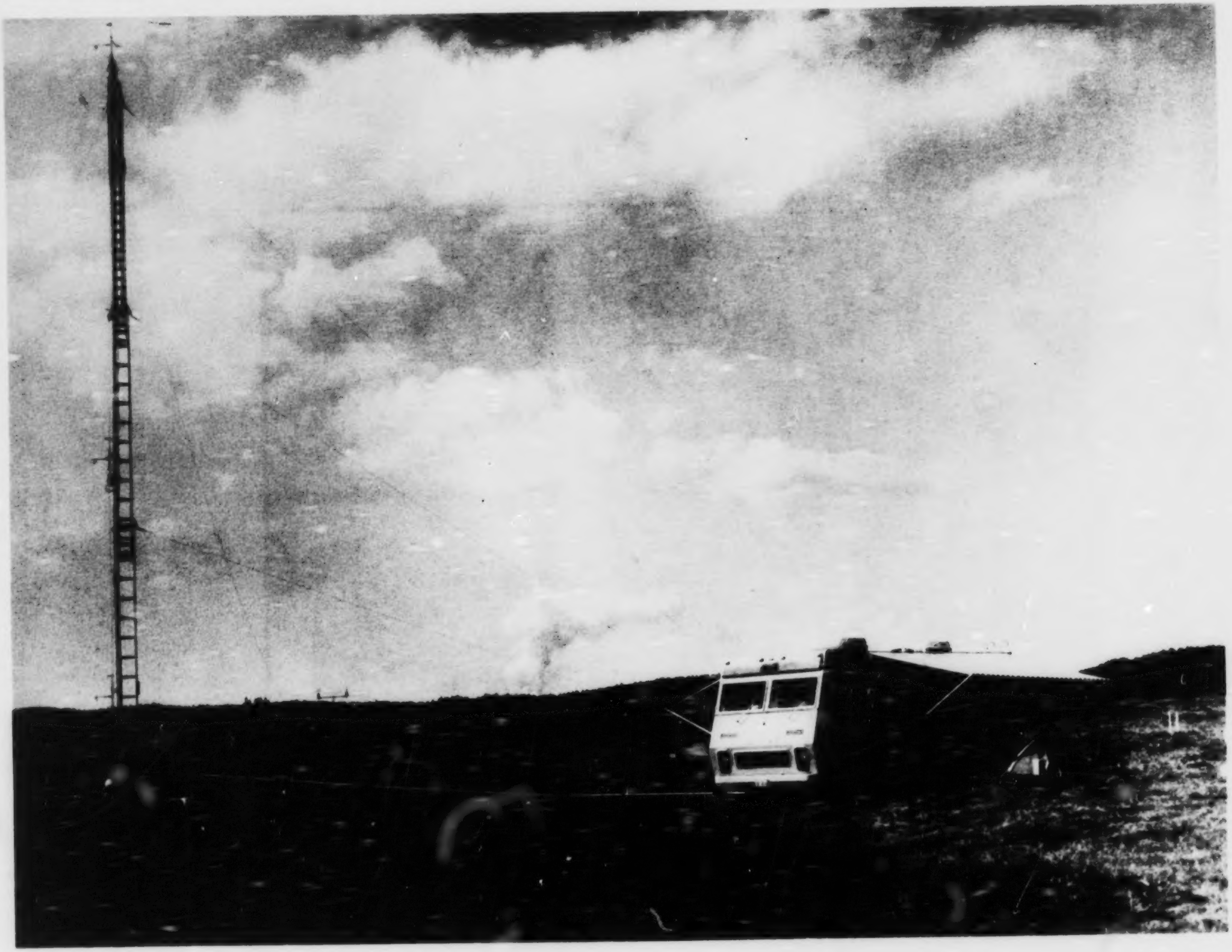

FIGURE 2. VIEW OF INSTRUMENTED TOWER AND MOBILE VAN WITH COOLING TOWER PLUME IN BACKGROUND.

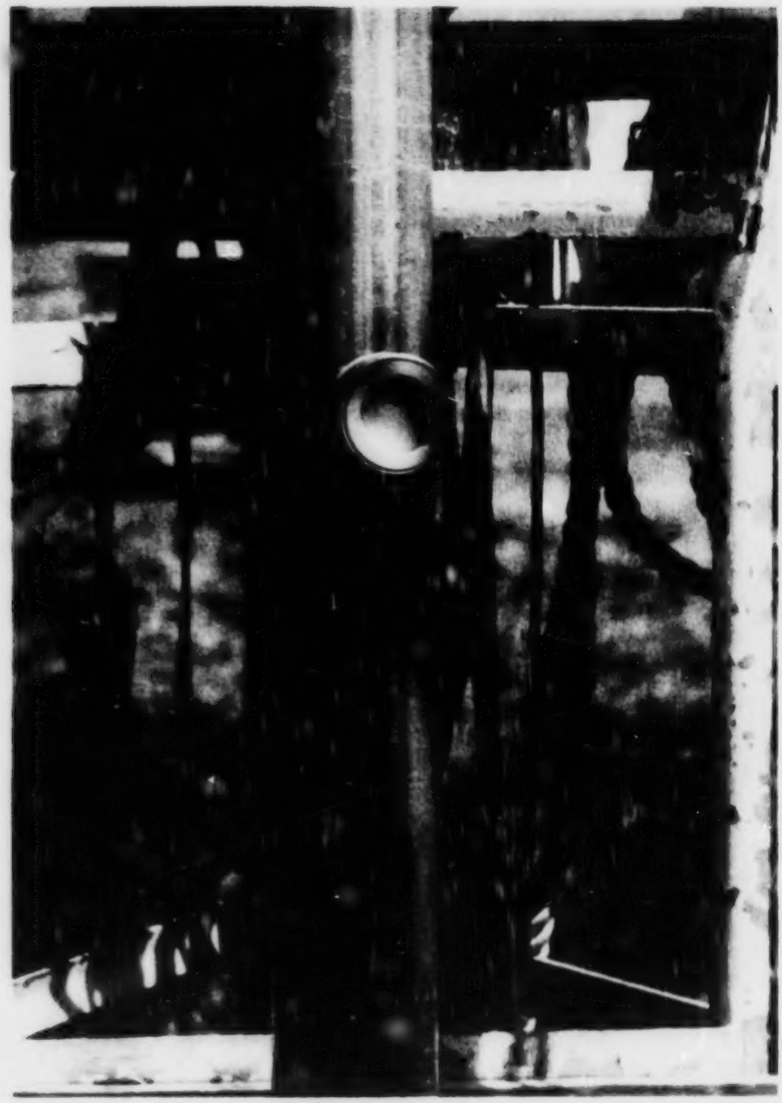

FIGURE 3. NUCLEPORE FILTER MOUNTED ON TOWER.

A 17 m crankup triangular tower was used to mount sensors and sample input lines. The gas and aerosol systems required inputs from various heights. Three heights, 0.91, 6.1, and 15.2 meters are used for intakes in the fixed height applications. Separate sampling lines, flow meters and pumps were used for each height. A single input tube, flow meter, and pump was used in applications requiring a single direct input.

Aerosol System

Aerosol samples were collected in the field for subsequent laboratory analysis. Samples were collected on nuclepore filters with a pore diameter of 0.8 μm. Moderate rates were employed to minimize sub-isokinetic sampling errors. Stainless steel filter holders with an effective collection area of 11.4 cm^2 were used. Figure 3 shows a filter mount, and a filter at the 0.91 m measurement height. Other filters are at 6.1 and 15.2 m. Air was drawn through the nuclepore filters for 1 to 3 hours at each of the three levels. The samples were analyzed for sulfur and lead by dispersion x-ray fluorescence. The combination of a species density on a filter and the total volume of air sampled were used to calculate the air concentration.

The flow rates through the sampling system were monitored by ROOTS flow meters (model 1.5M125). There are positive displacement meters that accurately measure the volume passing through the meter at a given temperature and pressure. If the sample is heated or cooled, its density changes as does the volume indicated. One temperature-compensated unit was obtained for initial testing. The variation did not appear to justify the use of such a unit in the current application. Running under identical conditions uncompensated meters gave essentially identical results for time periods and flow rates comparable to the current application. In addition, the three flow meters were tested by running them in various orders in series. The calibration differences were found to be negligible. The flow meters produce a signal for an event recorder each time 0.028 m^3 (1 cu ft) of air passes through. The ROOTS meter output from all three units was recorded on the same recorder to allow close comparison of both total flow and flow rate changes during experiments.

Gas - General

Three basic designs were proposed for the gas sampling effort; System A - Alternating Collector Bags, System B - Direct Sampling, and System C - Integrated Systems. These are shown diagramatically in Figure 4, and were tested in varying configurations as described below.

Each of the systems in Figure 4 has its own inherent advantages and disadvantages. The use of the alternative collector bag system can give a sample representative of the entire period of time. However, storage of certain highly reactive gases such as O_3 and NO is not possible, so the technique cannot be applied to these gases. The direct sampling system, however, is designed for such reactive gases. The high flow rate in the sampling lines yields residence times on the order of a few seconds. Only a small portion of the gas flowing into the mobile laboratory is used for the actual analysis. The small residence time in the sample lines is inherent in both Systems A and B, and may be true in System C. System B can only give sequential samples from different intake lines in our present system; its limitation is a single analyzer for each of the gases. This disadvantage could be overcome by employing several analyzers, as did Whelpdale[48]. System B has the advantage of direct sampling with minimum storage time. This system was used in several modes of operation for SO_2, NO_x, NO and O_3 in the current field effort.

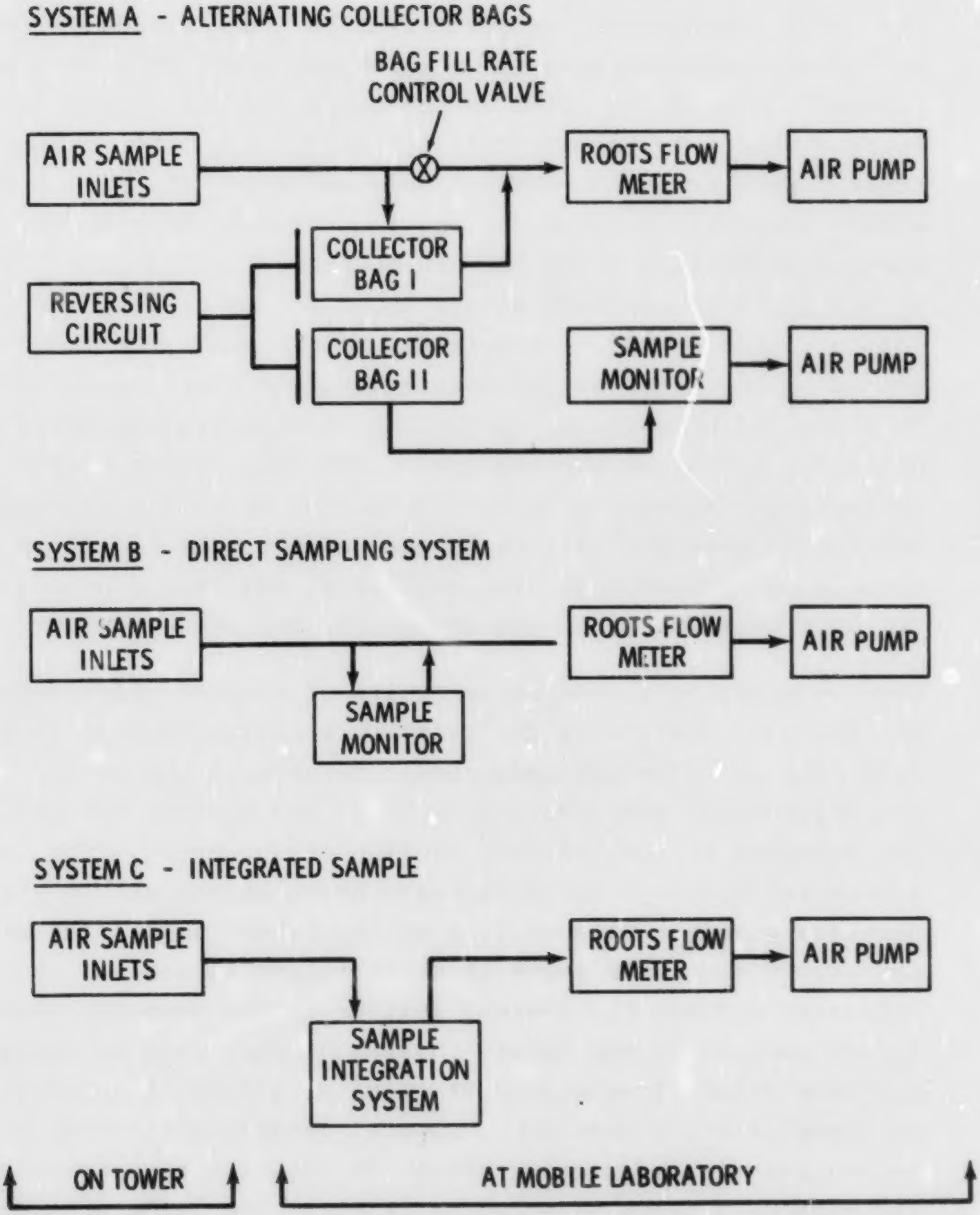
SYSTEM A - ALTERNATING COLLECTOR BAGS
BAG FILL RATE CONTROL VALVE
AIR SAMPLE INLETS
ROOTS FLOW METER
AIR PUMP
COLLECTOR BAG I
REVERSING CIRCUIT
COLLECTOR BAG II
SAMPLE MONITOR
AIR PUMP
SYSTEM B - DIRECT SAMPLING SYSTEM
AIR SAMPLE INLETS
ROOTS FLOW METER
AIR PUMP
SAMPLE MONITOR
SYSTEM C - INTEGRATED SAMPLE
AIR SAMPLE INLETS
ROOTS FLOW METER
AIR PUMP
SAMPLE INTEGRATION SYSTEM
ON TOWER
AT MOBILE LABORATORY

FIGURE 4. GAS SAMPLING SYSTEMS.

The third, integrated, sample system is most applicable for pollutant concentrations at or below the instrument detection limits. Although not used in the current field effort, preparations were made to test this system for SO_2. SO_2 deposition tubes[83] were prepared. These tubes use solid absorbents to effectively trap all the SO_2 passing through the tube at ambient conditions. The SO_2 can be thermally dissolved later. By purging a heated tube with a known volume of dry nitrogen into a collector bag, a sample may be prepared that is concentrated by the ratio of the volume used for sampling and purging. This ratio can be varied to provide concentrations within the detection limits of the analyzer. The lack of time and sufficiently favorable conditions during the field studies was the only reason this technique was not tested. Other techniques for concentrating samples of gas including SO_2 and NO_x were considered but not chosen for the present effort.

When considering the relative merits of each of these systems, an important feature is the relative accuracy that is attainable between different measurement heights on the tower, since the accuracy of the model to be developed depends directly on the accuracy of the vertical profile measurements. The use of a separate System A for each measurement height should yield accurate gradient data as long as the rates filling the bags are nearly equal and there is no differential loss of the pollutant between the systems (either in the sampling lines or during storage in the bags). System B, when used to sequence air flow intake from different heights, offers the potential for good relative accuracy. However several factors must be considered: a question arises in the time sequencing of the samples between measurement heights; the inlet pressure can affect the calibration of certain analyzers and switching between different inlet lines can change the pressure; slight absorbtion of the pollutant may occur in one line compared to another; the shock of connect-disconnect can have transient effects. Any of these could cause a spurious difference in readings between levels. An alternative might be to use a sampling system with a single sampling line. This would solve the problem of changes in sample lines. Any errors in the line would be the same for all heights. The sample intake line need only be long enough to reach between the different sampling levels on the tower. Current tests were performed by manually moving the line, although automation of such a system is not a difficult task[84,85].

The bag collection system appeared to be the most promising for SO_2 and NO_x measurements, although it was not used in the current field effort. We planned to use three system A sampling systems, one for each sampling height. Air samples would slowly fill the collector bags I for each height for periods on the order of 1/2 to 1 hour. Then, the plumbing would automatically switch collector bags I and II. Collector bags II would start to fill, while collector bags I were sequentially sampled by the SO_2 and NO_x analyzers. The collector bags I would then be emptied, purged with dry nitrogen and emptied, to prepare the system for another cycle of sampling.

The collector bags were specially fabricated out of Tedlar in a cube shape to permit maximum sample volume. Tedlar has acceptable properties for NO_x and SO_2 measurements. The collector bags were mounted inside a plexiglass box which sit inside a metal rack with a metal face in case of accident.

The sequencing of the system operated satisfactorily in each test at the laboratory. A FX system model programmable controller was used to control the sequencing. Stainless steel solenoid valves were used in all switching applications.

The bag collection system had a fault that precluded its use in the current field program. The boxes containing the collector bags imploded several times in mockup field tests in the mobile laboratory. The Tedlar bag was damaged in each implosion. Lowering the flow rate to the lowest acceptable sample line residence time was attempted, but the vacuum created was still sufficient to implode the box. As a result, this system was not available for the field tests.

In the field experiments, slightly different techniques were used for each gas. These are described along with the analysis method in the following section.

SO_2

Fixed tower heights and separate sampling lines were used for the SO_2 profile experiments. Samples from each height were sequenced as fast as possible through the SO_2 analyzer at a rate of about 1 every 2 minutes. A portable gas chromatograph manufactured by Analytical Instruments Development, Inc. (AID) was utilized. This instrument was modified with an electromechanical switch to automate the sampling procedure. The FX system programmable controller was used to sequence the sampling with other operations. The gas samples were sequenced through stainless steel and Teflon valves.

O_3

A flexible sample line was adopted for measuring the ozone profile. Ozone was determined using a Bendix Model 8002 Ozone Analyzer. The following description is taken directly from the Operation and Service Manual B1261TM, Bendix Process Instruments Division.

"The Bendix Model 8002 Ozone Analyzer operates over a wide range of temperature and humidity variations without adverse degradation to measurement accuracy. The system provides reliable operation and is designed for ease of maintenance. Electronic components are mounted on plug-in printed circuit cards, wherever practical, so that equipment operation can be restored quickly in the event of a component failure. Chemical and particulate filters, subject to periodic replacement, are mounted on the rear panel for ease of replacement.

The Ozone Analyzer provides a direct read-out of ozone concentration on a continuously exchanged ambient air sample. The system reacts quickly to quantitative changes in ozone content of the sample, while providing a highly stabilized measurement capability for extended periods, without repeated adjustments. In addition to the front panel meter indication, an output signal is provided through the front panel RECORDER jacks and rear panel terminal connections.

The Ozone Analyzer utilizes the principle of photometric detection of the chemiluminescence resulting from the flameless-gas-phase reaction of ethylene with ozone. This reaction produces light waves or photons that are transmitted to the photomultiplier tube. The photomultiplier tube converts the light waves into electrical energy. This electrical energy is multiplied or amplified by the photomultiplier tube, and is further amplified in the electrometer amplifier to provide the proper drive voltages for the front panel meter and the external strip-chart recorder. Thus, the resultant meter reading or the output to the recorder, is proportional to the light waves produced by the ozone-ethylene reaction. The degree of reaction is in turn proportional to the amount of ozone in the air sample.

The minimum performance parameters for the Ozone Analyzer are presented below. The instrument will operate within these stated performance parameters under the conditions listed.

a. Range: 0.01, 0.02, 0.05, 0.1, 0.2, 0.5, and 1 ppm full scale
b. Minimum detectable sensitivity: 1 ppb
c. Zero drift: ±1% per day to ±2% per three days
d. Span drift: ±1% per day to ±2% per three days
e. Precision: ±2% from mean value on the 0 to 0.1 ppm range
f. Linearity: ±0.5%
g. Noise: ≤±1% on the 0 to 0.1 ppm range with 10 second time constant
h. Interference equivalent: ≤0.01 ppm
i. Lag time: ≤3 seconds
j. Rise time: ≤7 seconds to reach 90% of ultimate indication
k. Fall time: ≤7 seconds to reach 90% of ultimate indication
l. Response time: ≤10 seconds to reach 90% of ultimate indication after input change (lag time plus response time)
m. Operational period: 7 or more days unattended
n. Ambient temperature fluctuations: ±5°C
o. Operating temperature extremes: 5°C and 40°C
p. Time constants: 1, 10 and 40 seconds
q. Power requirement: 105-125 volts, 60 Hz (to Hz optional), 350 watts
r. Outputs: 0 to 10 mV (recorder) and 0-1 Vdc (other outputs optional)."

NO_x/NO

The NO_x/NO instrument functions using chemiluminescence, a phenomenon in which light is produced as a byproduct of a chemical reaction. The intensity of the light produced is directly proportional to the concentration of the gas (NO) being measured, with the concentration of the other reactant (ozone) being held constant. Thus, the instrument provides for directing the sample gas into a reactor chamber. A selection is made on the front panel for the instrument to measure NO or NO_x. When NO_x is selected, the gas is directed into a catalytic converter that changes NO_x into NO. Ozone, generated within the instrument from the oxygen in ambient air, is also directed into the reactor chamber. The resulting chemical reaction in the reactor chamber produces light, which is sensed photoelectrically. The signal thus produced is amplified and drives a meter on the front panel. The meter indicates the concentration of NO or NO_x directly in ppm. The output is recorded on chart paper.

The specifications of the REM Model 642 NO and NO_x Monitor are given as follows:

Sensitivity:	5-ppb (S/N = 1 when C = 5-ppb).
Range:	0-.5, 0-2, 0-10 ppm.
Precision:	±1% of full scale.
Linearity:	1% for given range. ±1% of full scale between ranges.
Zero Drift:	±1% per day; ±2% per 3 days, ±3% per month.
Span Drift:	±1% per day; ±2% per 3 days, ±3% per month.
NO_2 to NO Converter:	Provides specific 100% conversion of NO_2 to NO.
Response Time: (10-90% of Steady State)	0-.5 ppm. RANGE: 15 Sec. 0-2, 0-10 RANGES: 9 Sec.
Reaction Chamber:	Operated at atmospheric pressure - no vacuum pump necessary.
Data Display:	Analog front panel meter, readout in parts per million. Digital voltmeter optional.

Data Output:	Front panel analog output terminals. Output voltage adjustable from 10 mv to 5 volts full scale on all ranges (100% overrange capability on analog output for each range).
Mode Control:	Manual front panel switch to change NO to NO_x mode. Remote mode switching optional. Automatic mode switching and determination of NO_2 concentration by difference method optional.
Zero Adjust:	Front panel 10-turn potentiometer.
Power Requirement:	350 Watts.
Operating Temperature:	Continuous duty at full load from 0 to 40C (32 to 104°F).
Inputs:	Separate sample and span/zero input selected by front panel switch.

Micrometeorology Data System

All components and location are shown in Figure 5.

Wind. Three dimension component wind speeds (G1, G2, G3) were measured at three heights (1.79, 7.77, and 17.1 m) by Gill UVW anemometers with shaft extensions. A detailed description of this system and its range of application may be found in references 84-88. The u and v component arms were pointed south and west respectively. The Gill wind data were recorded in digital form. The angle correction factors in reference 85 are used in the data reduction program to account for the "cosine" error.

Wind speed measurements at intermediate heights were obtained by cup sensors with the output recorded on strip chart recorders. Wind speed and direction were also monitored adjacent to the tower (15 m south) with a Climet Model

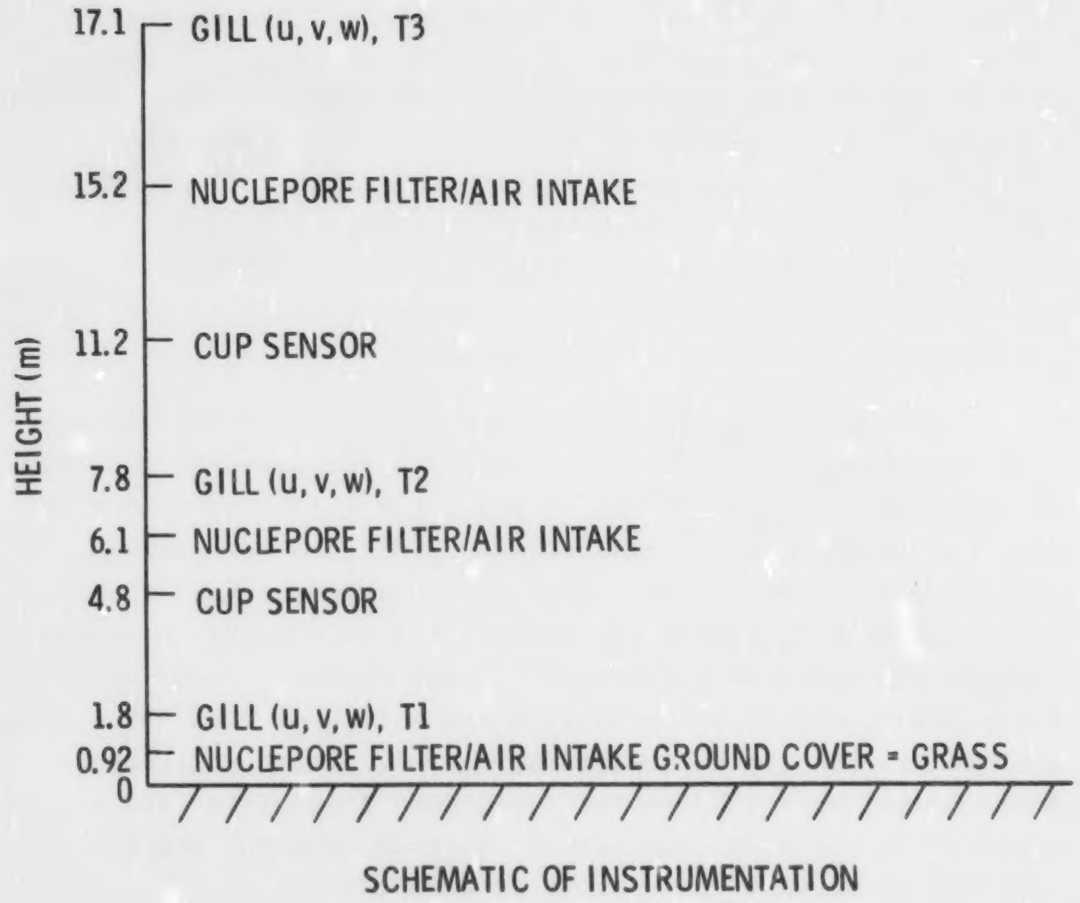
17.1
GILL (u, v, w), T3
15.2
NUCLEPORE FILTER/AIR INTAKE
11.2
CUP SENSOR
HEIGHT (m)
7.8
GILL (u, v, w), T2
6.1
NUCLEPORE FILTER/AIR INTAKE
4.8
CUP SENSOR
1.8
GILL (u, v, w), T1
0.92
NUCLEPORE FILTER/AIR INTAKE GROUND COVER = GRASS
0
SCHEMATIC OF INSTRUMENTATION

FIGURE 5. SCHEMATIC OF INSTRUMENTATION LOCATION.

weather vane and cup system. These were recorded on chart paper.

Air Temperature. The primary air temperature system (T1, T2, T3) used aspirated thermistor sensors at three heights. These were mounted in the lower portion of the Gill wind systems, and used bridge circuits with matched components. The multivolt output was recorded directly on the digital recording system. Each height has two identical but independent systems. The six thermistors were selected to matched resistance characteristics. The redundancy at each level provided additional field checks that circuit components were operating correctly. The time response of the thermistor in still air was about four seconds. The recorded values are changed to standard units as part of the computer program to reduce the data.

Additional onsite weather conditions were continually recorded using a hydrothermograph for temperature and relative humidity in a standard weather screen; a Solimeter (Model R401, Serial 134) for incoming solar radiation; a miniature net radiometer (Micromet Inst. Serial 276) for net radiation; a heat flux plate for heat flux into the ground; and barographs to record changes in atmospheric pressure. These were all recorded on chart paper, except net radiation and soil heat flux which were included in the digital recording system. These additional measurements were used in the field data acquisition and as independent checks on the primary systems data but are not reported as part of the current data set.

The digital recording system was a Metrodata Model digital tape recorder. Twenty channels of three decimal places and a sign were used. Data were recorded on a cassette tape at the rate of slightly over 2 sets per second. The contents of the channels are shown below.

Channel Content	Channel Content
	11 T 2
1, 2 HMS	12 T 2'
3 u 1	13 u 3
4 v 1	14 v 3
5 w 1	15 w 3
6 T 1	16 T 3
7 T 1	17 T 3
8 u 2	18 C
9 v 2	19 Tn
10 w 2	20 G/Ozone

Code for Channels

HMS hour, minute, seconds
+ u = south wind
+ v = west wind
+ w = wind upward
1 171 m
2 7.77 m
3 1.79 m
' second sensor system
C = Thermistor battery voltage
G = ground heat flux
Rn = net radiation

The Metrodata cassette data tapes were transferred to computer compatible tapes on a NOVA computer. Then an computer is used to reduce the data and provide appropriate summaries. Intermediate data translations by Metrodata and Battelle Columbus were necessary to recover the meteorology data.

SECTION VII

DATA COLLECTION

Field Tests

Brief field tests were performed to test instruments determining the vertical fluxes of SO_2, O_3, NO_x, NO, sulfur and lead. The instrumentation was described in the previous section. These tests were designed only to evaluate the operation of the equipment and demonstrate the possible resolution of deposition rates under field conditions. Extensive field data acquisition was not the goal of these experiments.

The site chosen was 10 km north of a fossil fuel plant at Centralia, Washington. The site elevation is approximately 85.3 meters (280 ft MSL), longitude 122° 55' 30" and latitude 46° 50' 5" N. The site is located near the center of T-16N, R-1-W block #25. Figure 6 summarizes the fetch in various directions around the site. A thirty degree sector is considered to be affected by the mobile laboratories (315 to 545°).

Figure 2 shows the site with the tower, instrumentation and mobile laboratory looking towards the Centralia plant. The cooling tower plume may be seen near the horizon.

The stack plume from the Centralia plant was not identifiable at the site during the tests of systems. Instead the tests were made on ambient pollutants from apparently more distant sources. The aerosol data has higher than normal copper values suggesting that some of the pollutants may be originating in the Tacoma area. This is consistent with wind trajectories.

A summary of field tests performed at this site is included in Table 3 with the date, time and purpose. The early tests in this table were valuable in evaluating the performance of the

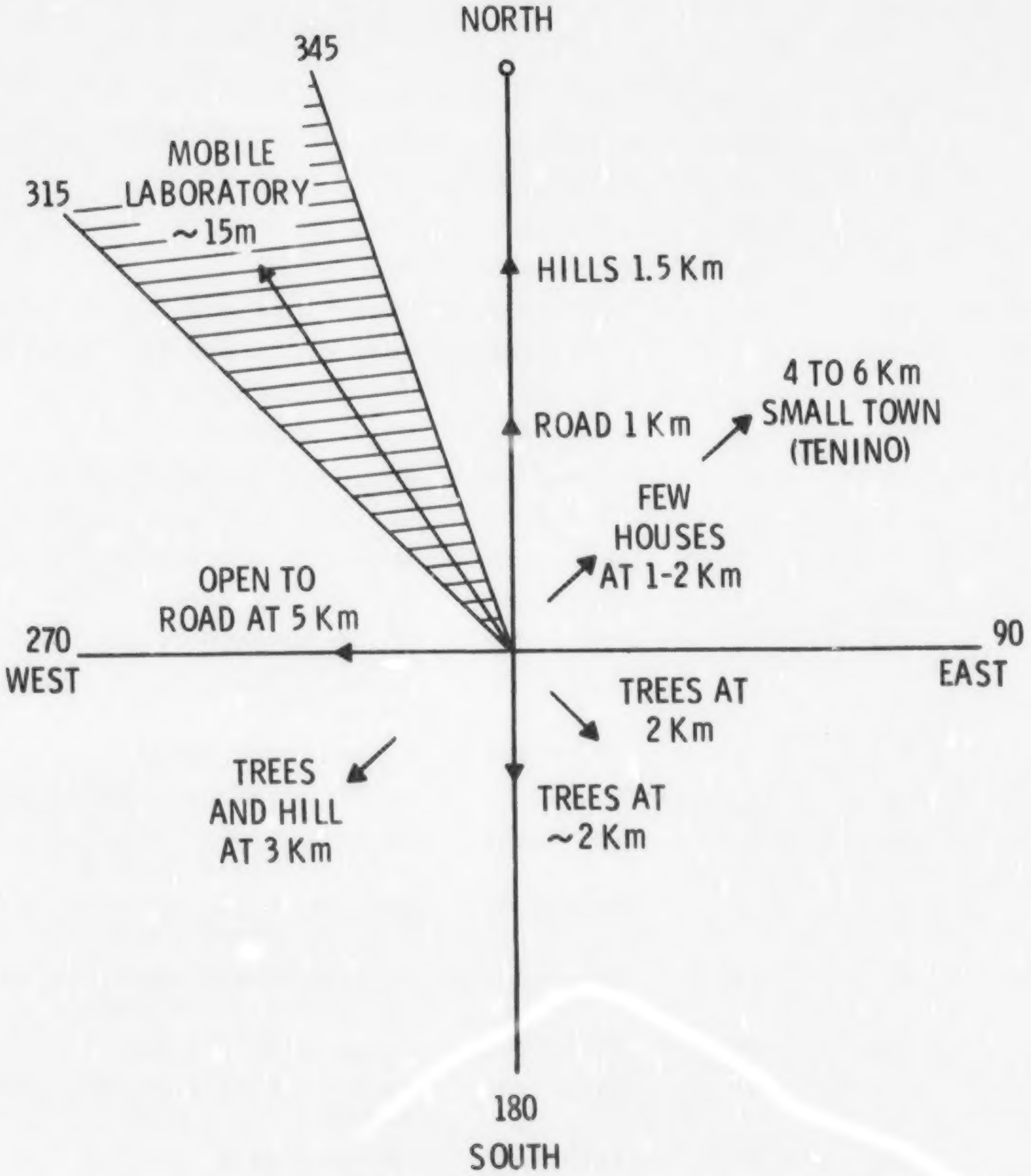
NORTH
345
315
MOBILE LABORATORY ~15m
HILLS 1.5 Km
4 TO 6 Km SMALL TOWN (TENINO)
ROAD 1 Km
FEW HOUSES AT 1-2 Km
OPEN TO ROAD AT 5 Km
270 WEST
90 EAST
TREES AT 2 Km
TREES AND HILL AT 3 Km
TREES AT ~2 Km
180 SOUTH

FIGURE 6. DIAGRAM OF FETCH AROUND SITE.
DISTANCES ARE NOT TO SCALE.

Table 3. SUMMARY OF FIELD TESTS DURING MARCH 1975 AT CENTRALIA.

Test #	Day of Month	Time	Purpose
1	12	1134-1332	Test aerosol system
2	12	1339-1429	Test ozone
3	12	1605-1825	Test ozone
4	12	1840-2029	Test ozone and SO_2 horizontal
5	12	2309-2355	Test ozone and SO_2 vertical
5b	13	0045-0311	SO_2 gradients
6	13	0715-0910	SO_2 gradients
7	13	1200-1315	SO_2, O_3, aerosol tests
8	13	1330-1358	SO_2, O_3, aerosol tests
9	13	1506-1546	SO_2, O_3, aerosol tests
10	13	2001-2045	O_3, SO_2 gradients fixed levels
11	14	0845-1020	SO_2 gradients fixed levels
12	14	1021-1123	Aerosol tests SO_2, O_3 middle level
13	14	1244-1420	O_3 at upper level
14	14	2030-2118	O_3 SO_2 gradients fixed levels
15	15	0317-0417	SO_2, O_3 times manually extended, fixed levels
16	15	0340-0355	SO_2, O_3 times manually extended, fixed levels
17	15	0634-0805	SO_2, O_3 times manually extended, fixed levels
18	16	0555-0615	Ozone single line
19	16	1045-1223	Ozone single line/SO_2 product tests
20	16	1449-1608	Aerosol test
21	16-17	2322-0440	NO_x/NO tests
22	17	0836-1026	SO_2 gradients, fixed levels
23	17	0909-1345	NO_x/NO gradient tests
24	17	1320-1350	Calibration tests

sampling and analysis systems and development of data acquisition procedures, but relatively few of these experiments are acceptable for complete analysis. During many of these tests the winds were unacceptable (i.e., from the mobile van direction, or a poor response direction for the wind system) or some other ambient condition was unsatisfactory. The tests revealed many factors relating to the potential performance of systems under field conditions. Once a system appeared to be operating satisfactorily, several experiments suitable for dry deposition determinations were performed as ambient conditions allowed.

The aerosol system operated as expected. The systems were leak tested by sealing the input ports on the tower and checking for flow. For each run nuclepore filters were mounted on the inlet ports. Air was drawn through the filters for identical periods while simultaneous micrometeorological data were collected. Some difficulty was encountered in matching the flow rates. The pump pressures were matched before starting the flow through the filters in each experiment. It was noted that during the experiments the middle level indicated consistently lower flows than the other levels. Attempts to match the flow were only successful in the last aerosol experiment.

The gas measurement system required considerable development during the field experiments. Ozone was destroyed or absorbed by the solenoid valves, so the automatic switching system was useless. The solenoid valves decreased the O_3 concentration by an order of magnitude. It was assumed that SO_2, NO_x, and NO could not be safely switched by these solenoids without considerable further testing.

A stainless steel Teflon ball-valve system was tested for switching the gases. Ozone was still removed, but at a lower rate. An attempt was made to "saturate" the system by running ozone from the ozone calibration instrument through the valves for a day. Tests just after this procedure indicated that measurable O_3 decay was no longer taking place. Several sets of vertical gradients were taken which looked promising. However, tests several days later indicated unrealistic gradients. The valves were tested again and found to be removing much of the ozone. It was concluded these valves could not be used for switching ozone. Additional tests showed that even the stainless steel Swage lock fittings were destroying enough ozone to produce significant differences between the fixed input lines. A single line system was tested for ozone profiles and found to give consistently reasonable results. Problems of matching flows and of differential loss in the intake lines were thereby avoided.

The ball-valves were tested for absorption of SO_2. The results indicated that no significant absorption was occurring. Fixed height profiles of SO_2 were taken whenever the meteorological conditions allowed. The SO_2 from the various intake lines was manually switched by the ball valves. The SO_2 levels were normally near or below the threshold of the instrumentation during the field effort.

The ozone generator in the REM NO_x/NO monitor failed at the beginning of the field effort. A replacement was obtained as quickly as possible and the NO_x, NO instrumentation was tested during the final days of the field effort. Data for both ball-valve switching of the fixed levels and single line profile were obtained.

SECTION VIII

RESULTS

The purpose of the current tests is to study the feasibility of using the surface flux profile method to determine atmospheric removal rates under field conditions. This involves the logistics of the instrumentation and data collection described in the preceeding sections. The ultimate proof is the demonstration of the ability to compute deposition rates using these systems. In certain situations, such as rainfall or very high humidities, certain of the experiments are obviously excluded and data are not collected. Less obvious excluding cases occur when conditions appear to be favorable, but the limitations of the instrumentation preclude determination of an accurate removal rate. This applies to both the meteorological and pollutant data acquisition systems. To demonstrate the magnitude of the errors under various conditions, the experimental accuracy will be estimated for the field data tests.

As a result of the briefness and preliminary nature of the field effort, data will be included in the analysis which were taken under less than ideal conditions. These data will be valuable in assessing the overall capability of the system.

Aerosol

The five sets of three samples collected on nuclepore filters were analyzed for total sulfur and lead. The methodology development for this analysis was the responsibility of John Cooper at ORTEC. His report is attached as Appendix A. Based on his recommendation, the samples were analyzed for sulfur by two methods; Energy Dispersive X-Ray Fluorescence analysis performed at ORTEC and Wavelength Dispersion X-ray Fluorescence analysis performed by Ben Paris at Battelle Columbus Laboratory.

John Cooper's results are included in Appendix A and the Battelle Columbus results in Appendix B .

The results are summarized for total sulfur in Table 4. The first two columns are the results supplied by Cooper and Paris. The last two columns are these values normalized to the reading at the top level. There is a close correspondence of the relative values between levels for the sulfur concentrations. The BCL summary does not include lead data.

The aerosol data for sulfur and lead from John Cooper (Appendix A) and uncorrected flow rates are given in Table 5. These are the raw data for computation of air concentrations. The flow rates need to be adjusted for the reduced pressures under which the volume flow rate was obtained.

Table 5 contains the air concentrations of the aerosols computed by two assumptions; equal internal pressure on all three lines in each experiment and different internal pressure in each line. Both assumptions are included because of the uncertainty involved in the pressure-temperature correction factors for the volume of air measured in each line. These factors are based on an empirical relationship for the correction determined in laboratory tests based on flow rates for a short intake line with a nuclepore filter. The correction factor derivation was performed for flow greater than 3×10^{-3} m^3/sec. Values below this are based on extrapolation of higher values.

Table 6 lists the correction factors for raw flow rate as a function of adjusted flow rate. These were used to determine specific correction factors in Table 5. The correction must be considered approximate because other influences such as lengths of lines, number of fittings and variations between laboratory and field conditions were not included.

Table 4. TOTAL AND NORMALIZED SULFUR AEROSOL CONCENTRATIONS UNCORRECTED FOR FLOW RATE.

Sample	Cooper (Appendix A) μg/cm^2	Paris (Appendix B) Total μg	Cooper ÷#3	Paris ÷#3
M1 3	1.29 ± .02	4.0	1.00	1.00
2	1.27 ± .02	3.8	.98	.95
1	1.43 ± .02	4.2	1.11	1.05
M7 3	2.25 ± .02	6.7	1.00	1.00
2	2.18 ± .02	6.4	.97	.96
1	2.56 ± .02	7.4	1.14	1.10
M8 3	2.81 ± .02	7.6	1.00	1.00
2	2.79 ± .02	7.8	.99	1.03
1	3.02 ± .02	8.7	1.07	1.08
M12 3	2.33 ± .02	6.7	1.00	1.00
2	2.34 ± .02	6.7	1.00	1.00
1	2.64 ± .02	7.4	1.13	1.10
M23 3	0.45 ± .02	1.9	1.00	1.00
2	0.46 ± .02	2.1	1.02	1.11
1	0.41 ± .02	2.1	.91	1.11

Table 5. SUMMARY OF COMPUTED AEROSOL AIR CONCENTRATIONS[1]

Run No.	Height (m)	Sample Rate (m^3/s) ($x10^3$)		Sulfur Air Concentrations[2] $\mu g/m^3$		Lead Air Concentrations[2] $\mu g/m^3$	
M-1	15.2	2.07[3]	2.06[4]	.613[3]	0.616[4]	0.23[3]	0.231[4]
	6.1	1.84	1.95	.681	0.641	0.25	0.237
	.914	2.25	2.15	.626	0.656	0.29	0.301
M-7	15.2	1.63	1.60	2.43	2.47	0.67	0.68
	6.1	1.37	1.48	2.80	2.60	0.80	0.74
	.914	1.71	1.63	2.62	2.76	0.69	0.72
M-8	15.2	2.19	2.18	6.00	6.02	1.22	1.22
	6.1	2.00	2.08	6.57	6.31	1.39	1.34
	.914	2.31	2.23	6.18	6.39	1.21	1.25
M-12	15.2	1.32	1.32	1.55	1.55	0.33	0.33
	6.1	1.15	1.18	1.78	1.73	0.33	0.32
	.914	1.44	1.41	1.60	1.64	0.29	0.30
M-23	15.2	1.99	2.08	0.333	0.319	0.37	0.35
	6.1	2.24	2.20	0.343	0.349	0.28	0.29
	.914	2.26	2.21	0.343	0.351	0.29	0.30

[1] The accuracy of these data is uncertain, so three places are listed recognizing that the actual accuracy may be less than this.

[2] based on a filter area of 7.92 cm^2.

[3] equal internal pressure assumed for all three lines in each run (average raw flow rate used).

[4] different internal pressures assumed for each sample line (raw flow rate used).

Table 6. FLOW RATE ADJUSTMENT (m^3s^{-1}).

Raw Flow Rate	Adjusted Flow Rate
1.00 x 10-3	1.00 x 10-3
1.50 x 10-3	1.39 x 10-3
2.00 x 10-3	1.58 x 10-3
2.50 x 10-3	1.73 x 10-3
3.00 x 10-3	1.94 x 10-3
3.50 x 10-3	2.08 x 10-3
4.00 x 10-3	2.22 x 10-3
4.50 x 10-3	2.34 x 10-3

SO_2

Table 7 contains the average air concentrations of SO_2 measured in three tests in the field. The data, time and run number are listed on the left. The average air concentrations in ppb along with standard deviations and number of points are given for the indicated levels. The small number of measurements at each level combined with the large standard deviation limits the accuracy of the profiles. The differences between levels can be expected to be more accurate than indicated by the standard deviations. These standard deviations include the effect of natural scatter as well as trends in the concentrations.

The least squares coefficients for all three data sets are given in Table 8. In all tests, the best fit profiles indicate deposition of SO_2. Only in run 2 are the gradients consistent with a reasonable log profile and large enough to be considered significantly non-zero gradients. The other two tests have very small gradients.

Table 7. SUMMARY OF SO_2 DATA RESULTS.*

Run	Date	Time	(0.91 m) Level 1	(6.1 m) Level 2	(15 m) Level 3
1	051375	1330-1358	2.4 ± .2(4)	2.5 ± .2(6)	2.3 ± .2(4)
2	051375	1506-1546	3.8 ± .4(5)	4.3 ± .7(8)	4.5 ± .5(4)
3	051676	1100-1214	4.5 ± .6(18)	-----	4.5 ± .5(17)

*Each set has the average concentration, its standard deviation in ppb and the number of points used.in para

Table 8. LEAST SQUARES TO SO_2 DATA.*

Run	B	m
1	2.38	.00276
2	3.86	.251
3	4.48	.0142

*χ = mlnz+B, z in meters.

NO_x, NO

The NO_x and NO profile experimental results are summarized in Tables 9 and 10. The run number data, starting time, and duration of the run are given on the left. The averages, standard deviations and number of points are also shown for each of the indicated levels. These average values are stated to ±0.1 ppb although the excepted absolute accuracy of chemiluminenscent instruments are an order of magnitude less accurate. The current interest is in relative accuracy between values which may be up to an order of magnitude better than absolute accuracy. The last column is the ratio of the concentration gradient to the upper level concentration multiplied by 100. Both short and long duration tests were run. The recording level was switched every 3 to 4 minutes. One minute average last value readings were taken off the chart. The last value was defined as the one minute period just before the level was changed. This should be the best value in terms of instrumental equilibrium. Table 11 contains a series of NO_x profiles computed from intermediate one-minute values read in the 0909-0948 run.

Ozone

The ozone profile results are given in Table 12. These results are all based on the roving line system, allowing at least two minutes for an equilibrium reading at each level. The data and time for each experiment are given on the left. The runs are numbered for later reference. After each average value the standard deviation and number of points are listed. The accuracy retained in this table is an order of magnitude better than the stated accuracy of the ozone monitor (± 0.001 ppm). This reflects both the fact these are average values and the current interest in relative values. The linear regression coefficients for these data are given in Table 13.

Table 9. SUMMARY OF NO_x PROFILE RESULTS.*

Run	Date	Time Start	Duration (min)	Heights (m) 0.304	7.62	%Δ
1	051675	2322	6	51.3 ± 3.8 (6)	50.7 ± 4.3 (5)	1.3
2	051675	2340	44	15.6 ± 2.5 (15)	15.3 ± 2.9 (16)	1.8
3	051775	0419	21	4.4 ± 1.1 (10)	4.5 ± 0.9 (10)	-1.7
4	051775	0909	36	18.9 ± 1.4 (6)	20.1 ± 2.1 (5)	-6.2
5	051775	0945	41	22.3 ± 3.7 (5)	23.4 ± 2.5 (6)	-4.9
6	051775	1139	36	30.7 ± .7 (26)	31.1 ± 0.7 (20)	-1.4

*Each set has the average air concentration in ppb, the standard deviation, and the number of values in para. The reason for retension of ±0.1 ppb accuracy is explained in the text. The %Δ column is the vertical percentage change in concentration relative to the upper level concentration.

Table 10. SUMMARY OF NO PROFILE RESULTS.*

				Heights (m)				
				0.304		7.62		
Run	Date	Time Start	Duration (min)					%
1	051675	2332	8	6.1	1.9(4)	6.7	1.6(3)	-9.5
2	051775	1215	17	18.7	5.2(5)	19.1	5.0(4)	-2.1
3	051775	1322	12	23.0	4.1(4)	24.4	3.9(3)	-5.8

*Each set has the average concentration in ppb, the standard deviation and the number of values. See text for reason for retention of 0.1 ppb accuracy. The % column is the ratio of the difference of the concentrations to the upper level concentration multiplied by 100.

Table 11. SUMMARY OF VARIATION NOTED IN NO_x PROFILE DATA AT 0909-0948.

Height	.304m	7.62m	% Change
Last values	11.9	20.1	-6.2
Second last values	19.3	20.0	-3.5
Third last values	18.5	19.8	-4.0

*All values are NO_x air concentrations in ppb.

Table 12. OZONE PROFILE SUMMARY*.

Date	Time	Run	Heights 0.304m	 2.44m	 7.62m
051775	0355-500	#1	0.0217 ± .0023(15)	no data	0.0249
051775	0504-525	#2	0.0217 ± .0008(3)	0.0231 ± .0010(6)	0.0241 ± .0018(2)
051775	0836-930	#3	0.0351 ± .0033(6)	0.0372 ± .0034(13)	0.0372 ± .0033(7)
051775	0930-1030	#4	0.0392 ± .0010(9)	0.0403 ± .0010(15)	0.0407 ± .0012(8)
051775	1139-1225	#5	0.0442 ± .0014(6)	0.0449 ± .0014(14)	0.0455 ± .0017(7)
051775	1226-1320	#6	0.0435 ± .0015(8)	0.0448 ± .0016(15)	0.0456 ± .0013(7)

*Values in ppm with standard deviation and number of data points after each value. See text for reason for retention of ±0.0001 ppm.

Table 13. LEAST SQUARES FIT TO OZONE DATA*.

Run #	B	m
1	.0229	.000993
2	.0225	.000736
3	.0361	.000696
4	.0398	.000473
5	.0447	.000362
6	.0443	.000648

*$\chi = m(\ln z)+B$, where χ = concentration in ppm and z is height in meters

Meteorological Data

Meteorological data collected during the field tests were reduced and summarized for the periods of interest. Tables 14 thru 19 contain these results for the experiments identified for possible deposition computations in the previous sections. Each table is labeled relative to the applicable experiments. The averages of wind speed ($\overline{u}$), vertical velocity ($\overline{w}$), products of wind speed and vertical velocity ($\overline{uw}$), air temperature ($\overline{T}$) and products of air temperature and vertical velocity ($\overline{\Theta w}$) are given as a function of measurement height; 3 = upper level, 2 = middle level, 1 = lower level. Omitted lower level values do not apply to the current analysis. Notation is made of the wind direction mode with the extremes on both sides in ten degree sector units. Also listed are the gradients of temperature and wind speed, as well as the Richardson number; all based on levels 1 and 3. The $\overline{\Theta w}$ values are based on w lagged 2.0 seconds to allow for the Θ response time.

Table 14. SUMMARY OF METEOROLOGICAL DATA FOR SO_2 RUNS 1-3.*

SO_2 Run#	Height (m)	$\overline{u}$ (m/s)	$\overline{w}$ (m/s)	$\overline{uw}$ (m^2/s^2)	$\overline{T}$ (°C)	$\overline{w\Theta}$ (°A m/s)	Notes
1 (28 min)	3	4.29	-.060	-.307	20.69	-17.8	DM = 300° - 330° - 010°
	2	3.70	.036	.0445	21.09	-	DT = .0605 °C/m
	1	3.30	.061	-	21.76	-	DU = .0647 m/s m
							RI = .482
2 (40 min)	3	3.12	-.026	-.153	23.11	- 7.87	DM = 300° - 320° - 40°
	2	2.69	.039	-.024	23.51		DT = .0584
	1	2.47	.048	-	24.15		DU = .0425
							RI = 1.07
3 (74 min)	3	2.24	.043	.113	14.08	12.5	DM = 20° - 150° - 260°
	2	1.92	.050	.0929	14.17	-	DT = -.0411
	1	1.70	.060	-	14.86	-	DU = .0357
							RI = -1.10

*$\overline{u}$ is mean wind speed, $\overline{w}$ is mean vertical velocity, $\overline{uw}$ is the average of the products of u and w, $\overline{T}$ is the mean air temperature, $\overline{w\Theta}$ is the average product of W and T, DM are the extremes of wind direction with the mode in the middle, DT and DU are average temperature and wind speed gradients, RI is Richardson number. DU, DT and RI are defined by heights 1 and 3.

Table 15. SUMMARY OF METEOROLOGICAL DATA FOR NO_x RUNS 1-3.*

NO_x Run#	Height (m)	$\overline{u}$ (m/s)	$\overline{w}$ (m/s)	$\overline{uw}$ (m^2/s^2)	$\overline{T}$ (°C)	$\overline{w\Theta}$ (°A m/s)	Notes
1 (6 min)	1	3.47	.071	.242	9.33	19.7	DM = 30° - 100° - 120°
	2	2.88	.080	.194	9.44	-	DT = .0045 °c/m
	3	2.24	.100	-	9.41	-	DU = .0813 m/s m
							RI = .0236
2 (33 min)	1	2.67	.049	.133	9.29	13.7	DM = 90° - 120° - 150°
	2	2.32	.054	.127	9.36	-	DT = .0132
	3	1.76	.079	-	9.24	-	DU =
							RI = .129
3 (21 min)	1	2.29	.043	.0951	7.45	12.1	DM = 140° - 180° - 190
	2	1.91	.034	.0648	7.18	-	DT = .0755
	3	1.16	.036	-	6.45	-	DU = .0742
							RI = .480

*Notation is defined in Table 14.

Table 16. SUMMARY OF METEOROLOGICAL DATA FOR NO_x RUNS 4-6.*

NO_x Run#	Height (m)	$\overline{u}$ (m/s)	$\overline{w}$ (m/s)	$\overline{uw}$ (m^2/s^2)	$\overline{T}$ (°C)	$\overline{w\Theta}$ (°A m/s)	Notes
4 (35 min)	1	1.76	.018	.0789	10.95	5.27	DM = 90° - 130° - 270°
	2	1.59	.052	.110	11.02	-	DT = -.0210 °c/m
	3	1.49	.090	-	11.42	-	DU = .0179 m/s m
							RI = -2.26
5 (38 min)	1	1.90	.049	.0905	11.86	14.0	DM = 60° - 180° - 230°
	2	1.70	.047	.0679	11.91	-	DT = -.0260
	3	1.31	.083	-	12.40	-	DU = .0252
							RI = -1.41
6 (36 min)	1	2.21	.019	.0355	14.18	5.64	DM = 90° - 150° - 230°
	2	1.99	.050	.0955	14.13	-	DT = -.0323
							DU = .0278
							RI = -1.43

*Notation is the same as Table 14.

Table 17. SUMMARY OF METEOROLOGICAL DATA FOR NO RUNS 1-3.*

NO Run#	Height (m)	$\overline{u}$ (m/s)	$\overline{w}$ (m/s)	$\overline{uw}$ (m^2/s^2)	$\overline{T}$ (°C)	$\overline{w\theta}$ (°A m/s)	Notes
1 (8 min)	1	3.31	.018	.0502	9.33	4.98	DM = 70° - 100° - 120°
	2	2.76	.053	.119	9.44	-	DT = .0775 °c/m
	3	2.12	.080	-	9.40	-	DU = .00506 m/s m
							RI = .0292
2 (17 min)	1	2.44	-.019	.0239	14.79	-5.72	DM = 70° - 130° - 22°
	2	2.05	.036	.0654	14.79	-	DT = -.0361
	3	1.78	.095	-	15.48	-	DU = .0439
							RI = -.640
3 (12 min)	1	2.20	.020	.102	16.19	6.17	DM = 0° - 110° - 180°
	2	1.75	.040	.0598	16.17	-	DT = -.0336
	3	1.54	.082	-	16.85	-	DU = .0433
							RI = -.606

*Notation is defined in Table 14.

Table 18. SUMMARY OF METEOROLOGICAL DATA FOR O_3 RUNS 1-3.*

O_3 Run#	Height (m)	$\overline{u}$ (m/s)	$\overline{w}$ (m/s)	$\overline{uw}$ (m^2/s^2)	$\overline{T}$ (°C)	$\overline{w\Theta}$ (°A m/s)	Notes
1 (65 min)	1	2.18	.062	.138	7.48	17.4	DM = 100° - 180° - 230° DT = .0626 °c/m DU = .0684 m/s m RI = .468
	2	1.80	.036	.066	7.24	-	
	3	1.13	.040	-	6.68	-	
2 (21 min)	1	3.27	.192	.628	7.73	53.8	DM = 160° - 200° - 210° DT = .0448 DU = .0946 RI = .175
	2	2.86	.093	.261	7.48	-	
	3	1.83	.097	.171	7.19	-	
3	1	2.04	.051	.129	10.42	14.4	DM = 80° - 130° - 230° DT = -.0191 DU = .0267 RI = -.925
	2	1.82	.066	.128	10.51	-	
	3	1.63	.092	.156	10.86	-	

*Notation is defined in Table 14.

Table 19. SUMMARY OF METEOROLOGICAL DATA FOR O_3 RUNS 4-6.*

O_3 Run#	Height (m)	$\overline{u}$ (m/s)	$\overline{w}$ (m/s)	$\overline{uw}$ (m^2/s^2)	$\overline{T}$ (°C)	$\overline{w\Theta}$ (°A m/s)	Notes
4 (60 min)	1	1.82	.032	.0797	11.77	9.01	DM = 20° - 160° - 270° DT = -.0253 °c/m DU = .0243 m/s m RI = -1.47
	2	1.61	.048	.0793	11.82	-	
	3	1.45	.087	-	12.30	-	
5 (46 min)	1	2.21	-.007	-.0065	14.27	-1.96	DM = 80° - 130° - 220° DT = -.0310 DU = -.0294 RI = -1.22
	2	1.99	.032	.061	14.23	-	
	3	1.76	.103	-	14.89	-	
6	1	2.18	.017	.0383	15.44	5.13	DM = 20° - 130° - 300° DT = .0431 DU = .0405 RI = -.894
	2	1.85	.057	.113	15.47		
	3	1.56	.075	-	16.75		

*Notation is defined in Table 14.

Table 20 summarizes the diffusivities and their relative experimental accuracy. The resolution shows considerable variation and is generally poor. Several of the momentum values are significant, but all the heat values have such large experimental errors that they cannot be considered for computations.

Deposition Parameter Computations

Pollutant profiles and meteorological summaries given in preceeding sections are used for computation of deposition parameters. The computation is carried through to the final product in all cases to identify the sources and magnitude of experimental error. Anomalous results may be reasonable when the experimental accuracy is considered. More important, determining error magnitude clearly identifies the most reliable cases. It is in these latter cases where the results will demonstrate the consistency and applicability of the approach.

Separate tables of the deposition computations are given for each of the gases using the momentum eddy diffusivity (Tables 21 to 24). Run numbers on the left correspond to numbers identified in the previous sections for each gas. The fractional pollutant gradient values in the next columns on the left are computed from values taken directly from previous tables. The K_m and K_h columns contain eddy diffusivities adjusted linearly with height to correspond to the same geometric height as the pollutant concentration gradient. The V_m and V_h columns contain the computed values of deposition velocity using the previous columns. As noted earlier, estimates of experimental accuracy have been carried through the computation to identify the most reliable case. As noted, the accuracy of the gradients has been carried through with several values. One percent is the best value possible. The other values are given to demonstrate the change in reliance with

Table 20. COMPUTED EDDY DIFFUSIVITIES FOR MOMENTUM K_m AND SENSIBLE HEAT K_h AT 5.53m.

Gas	Run #	$\overline{K}_m(m^2/s)$	$\sigma_{K_m}(m^2/s)$	$K_h(m^2/s)$	$\sigma_{K_h}(m^2/s)$
SO_2	1	.767	.382	- 5.76	97.4
	1*	1.33	.257		
	2	1.65	.353	.431	.101E 03
	2*	2.18	.641		
	3	- .467	.389	-2.31	.140E 03
	3*	.843E-01	.802		
NO_x	1	.538E-01	.226	85.8	.160E 04
	1*	.340	.234		
	2	- .103	.200	7.40	.436E 03
	2*	- .282E-01	.174		
	3	.454E-01	.103	- .756E-01	74.4
	3*	.112E-02	.549E-01		
	4	-2.64	.827	1.38	.271E 03
	4*	-1.63	3.95		
	5	.103	.646	3.50	.220E 03
	5*	.378	.840		
	6	.233	.226	-6.13	.178E 03
	6*	.120	.999		
NO	1	.121	.534E-01	24.3	.113E 04
	1*	.255	.146		
	2	-1.60	.895E-01	-14.2	.160E 03
	2*	.186	.396		
	3	-1.34	.215	9.71	.172E 03
	3*	.290	.606		
O_3	1	- .415E-01	.167	- .499E-01	89.9
	1*	- .107E-01	.676E-01		
	2	- .248E-02	.830	-1.82	.130E 03
	2*	.621E-01	.132		
	3	- .935	.744	6.76	.300E 03
	3*	- .755E-01	1.25		
	4	- .883	.531	.433	.226E 03
	4*	- .904E-01	1.25		
	5	- .307	.605E-01	-1.40	.185E 03
	5*	.593E-01	.487		
	6	- .306E-01	.111	5.10	.134E 03
	6*	- .156	.541		

*meteorology data from middle and lower level used.

Table 21. DEPOSITION COMPUTATION FOR SO_2

Run#	f^1	$K_m{}^2$	V_{dm}	$\pm\sigma V_{dm}$ Profile Accuracy Assumption			
				1%	3%	5%	10%
	m^{-1}	$m^2\ s^{-1}$	$cm\ s^{-1}$	$cm\ s^{-1}$	$cm\ s^{-1}$	$cm\ s^{-1}$	$cm\ s^{-1}$
1	-2 ± 7	0.517 ± .335 1.33 ± .26	0.10 0.27	0.37 0.95	0.70 2.8	1.8 4.7	3.5 9.5
2	-109 ± 7	1.11 ± .24 2.18 ± .64	1.21 2.38	.27 .66	.35 .77	.47 .95	1.00 1.54
3	-6 ± 7	-0.314 ± .262 .084 ± .80	- .19 .05	.27 .81	.68 .85	1.12 .94	2.22 1.27

Footnotes:

[1] $f = \left(\frac{1}{\chi}\right)_{z_2} \times \left(\frac{\Delta\chi}{\Delta z}\right)_{z_1 z_2} \times 10^4$ where $z_1 = 0.914$ m and $z_2 = 15.2$ m. Accuracy is based on ±1% gradient error.

[2] Values of K_m adjusted to correspond to same heights as the pollutant gradients. The first K_m is based on the upper and lower level data and the second K_m is based on the middle and lower data.

Table 22. DEPOSITION COMPUTATION FOR NO_x

Run#	f^1	$K_m{}^2$	V_{dm}	$\pm\sigma_{V_{dm}}$ Profile Accuracy Assumption 1%	3%	5%	10%
	m^{-1}	$m^2\ s^{-1}$	$cm\ s^{-1}$	$cm\ s^{-1}$	$cm\ s^{-1}$	$cm\ s^{-1}$	$cm\ s^{-1}$
1	17 ± 14	+.014 ± .062	.00238	.011	.012	.014	.022
		+.139 ± .095	.0236	.025	.061	.100	.20
2	25 ± 14	-.028 ± .055	-.0070	.014	.018	.024	.042
		-.012 ± .071	-.0030	.018	.018	.020	.024
3	-24 ± 14	+.013 ± .028	.0031	.007	.009	.011	.019
		+.001 ± .022	.0002	.004	.004	.004	.005
4	-85 ± 14	-.73 ± .23	-.62	.22	.37	.55	1.04
		-.67 ±1.6	-.57	1.36	1.39	1.44	1.65
5	-68 ± 14	.03 ± .18	.02	.12	.12	.12	.13
		.15 ± .34	.02	.23	.23	.25	.31
6	-19 ± 14	.064 ± .062	.01	.012	.024	.038	.074
		.05 ± .41	.01	.082	.085	.084	.11

Footnotes:

[1] $f = \left.\frac{1}{\chi}\right|_{z_2} \times \left.\frac{\Delta\chi}{\Delta z}\right|_{z_1 z_2} \times 10^4$ where $z_1 = 0.304$ m and $z_2 = 7.62$ m. Accuracy is based on ±1% gradient error.

[2] Values of K_m are adjusted to correspond to the same height as the pollutant gradients. The first K_m for each run is based on the upper and lower level gradients, and the second K_m for each run is based on the middle and lower level data.

Table 23. DEPOSITION COMPUTATION FOR NO

Run#	f^1	K_m [2]	V_{dm}	$\pm\sigma_{V_{dm}}$ Profile Accuracy Assumption 1%	3%	5%	10%
	m^{-1}	$m^2\ s^{-1}$	$cm\ s^{-1}$	$cm\ s^{-1}$	$cm\ s^{-1}$	$cm\ s^{-1}$	$cm\ s^{-1}$
1	-129 ± 14	.033 ± .014	.043	.019	.023	.030	.050
		.104 ± .060	.13	.08	.09	1.11	.16
2	-294 ± 14	-.43 ± .024	-1.26	.09	.19	.31	.61
		.076 ± .162	.22	.48	.48	.48	.49
3	-789 ± 14	-.36 ± .06	-2.84	.48	.50	.54	.69
		-.118 ± .247	.931	1.95	1.95	1.95	1.96

Footnotes:

[1] $f = \frac{1}{\chi}\Big|_{z_2} \times \frac{\Delta\chi}{\Delta z}\Big|_{z_1 z_2} \times 10^4$ where $z_1 = 0.304$ m and $z_2 = 7.62$ m. Accuracy is based on ±1% gradient error.

[2] Values of K_m are adjusted to correspond to the same height as the pollutant gradients. The first K_m for each run is based on the upper and lower level data, and the second K_m for each run is based on the middle and lower level data.

Table 24. DEPOSITION COMPUTATION FOR O_3

Run#	f^1 m^{-1}	K_m[2] m^2 s^{-1}	V_{dm} cm s^{-1}	$\pm\sigma_{V_{dm}}$ Profile Accuracy Assumption 1% cm s^{-1}	3% cm s^{-1}	5% cm s^{-1}	10% cm s^{-1}
1	-176 ± 14	.011 ± .045 -.004 ± .028	.019 .007	.078 .049	.078 .049	.078 .049	.079 .049
2	-135 ± 14	-.001 ± .22 .025 ± .054	.001 .034	.22 .073	.22 .074	.22 .075	.22 .081
3	-81.7± 14	.253 ± .20 -.0311± .51	-.20 -.02	.17 .42	.19 .42	.24 .42	.39 .42
4	51.1 ± 14	-.24 ± .14 -.04 ± .51	-.12 -.02	.08 .26	.12 .26	.18 .26	.28 .27
5	-38.3 ± 14	-.083 ± .016 .024 ± .20	-.032 .01	.013 .03	.035 .08	.058 .13	.12 .25
6	-62.3 ± 14	-.008 ± .030 -.064 ± .22	-.005 -.04	.019 .14	.019 .14	.020 .14	.022 .16

Footnotes:

[1] $f = \frac{1}{\chi}\Big|_{z_2} \times \frac{\Delta\chi}{\Delta z}\Big|_{z_1 z_2} \times 10^4$ where z_1 = 0.304 m and z_2 = 7.62 m. Accuracy is based on ±1% gradient error.

[2] Values of K_m are adjusted to correspond to the same height as the pollutant gradients. The first K_m for each run is based on the upper and lower level data, and the second K_m for each run is based on the middle and lower level data.

the decrease in profile accuracy under various conditions. Using the best accuracy possible indicates the applicability of the methodology in a given situation; that is, if a certain percentage profile accuracy is too limiting, then the methodology cannot be realistically applied under that set of conditions. In many cases the relative accuracy is not as good as ±1%.

SECTION IX

DISCUSSION

Aerosol

The aerosol results obtained by two independent laboratories demonstrate that the necessary relative accuracy on the order of 1 to 2% of the concentrations has been achieved for the filter analysis. The relative accuracy applies in computing the deposition velocity. An actual aerosol flux computation will depend on the absolute accuracy of the pollutant concentration. The achievable accuracy is on the order of ± 20% with application of corrections not made in the current study. These results show a reasonable factor between the achievable absolute and relative accuracy in the filter concentration data.

Much of the consistent variation in the filter concentration data was traced to pressure variations within the air intake lines. These variations could not be adequately accounted for in the current tests. The pressure in the air intake lines is a function of the air temperature within the line, the air pump setting, the filter resistance to flow, and the air intake line resistance to flow. The latter varies with the length and size of the air line as well as the number of flow restrictive fittings in the air line. The flow rate-based correction factors for pressure within the lines accounts only for the relationship between the air pump setting and the filter resistance.

The sulfur aerosol air concentration is derived assuming two pressure correction factors. First the factor is based on the average flow rate for all three lines. This results in profiles that are as badly kinked as the raw data. Second, the factor is based on the actual flow rates for each data point. This results in reasonable vertical profiles. The computed air concentration decreases with height. This is felt to be a result of the shortcoming of the pressure correction factor. The suggested explanation is that the line pressure is significantly affected by factors such as the resistance to flow in the air intake line. In such case the pressure in the line is progressively overestimated from the bottom to the top data levels on the tower. This results in an underestimation of air concentration at higher tower levels, as a result of progressively greater overestimation of the total sample volume. Hence the profiles are not felt to be indicating either the direction or magnitude of sulfur aerosol removal, but rather a result of the pressure correction.

The comments on the sulfur aerosol results apply also to the lead aerosol results. The lead profiles appear to have considerably more scatter than the sulfur, and the implication is that they are not as accurate. Flow rate inaccuracy precluded deposition velocity computation in the current effort.

Meteorology

The use of the upper level of meteorology data for eddy flux computations is considered superior in most cases than is the middle level. The response time of the wind sensors for flux computations is less limiting at the upper level. Eddy flux estimates made using the middle level may have an additional source of error not considered in the estimates of experimental accuracy, this is the lack of response to higher frequency atmospheric motions. The error could be estimated and corrected by spectral analysis, but this was beyond the scope of the current effort. The upper level values are considered most reliable except when the constant flux surface layer appears to be below the upper level. Then the middle level is considered better.

Both the upper and middle levels were presented in the results. The values were consistent with larger experimental errors estimated for the middle level data. The large experimental errors in the eddy diffusivity determination are not suprising. A certain correspondence can be expected between the accuracy of the pollutant profiles and the eddy diffusivities. The conditions that lead to difficulties in accurate pollutant profile determination also lead to similar difficulties in accurate wind velocity profile determination. In addition, the eddy diffusivity determination requires direct flux estimates. This was the major source of error in many cases in the current results. The low accuracy of a term resulting from the substraction of two numbers of near equal magnitude occurred in all the heat computations.

Gases

$\underline{SO_2}$. The SO_2 profiles were summarized in Tables 7 and 8 in Section VII. Although the gradients are negative in all cases, only in Run #2 is it significantly non-zero. This is reflected in the large estimated errors in the deposition velocities even at the 1% assumed profile accuracy compared to the computed deposition velocity for Runs #1 and 3 in Table 21. The magnitude of the error is the same for Run #2, but the relative accuracy is much better. Runs 1 and 2 had significant winds from the mobile van sector direction. The results must be considered suspect since the mobile van may influence both pollutant and wind characteristics at the tower.

The deposition velocity obtained for Run #2 has a reasonable magnitude based on previously determined values as well as an experimental accuracy that is within reasonable limits. For this case the "aerodynamic" deposition velocity (using Equation 14) is 2.2 cm/s. In terms of resistances to SO_2 flux these produce 0.44, 0.90, and .46 s/cm for the atmospheric (inverse of aerodynamic resistance), total resistance (inverse of computed V_d), and surface resistance (difference of first two). The surface and atmospheric terms are nearly equal in this case.

NO_x, NO and O_3. The NO_x and NO results and notes were summarized in Tables 9 and 10. A number of short experiments during the night are included along with longer tests. These former were part of the NO_x, NO system shake-down and were not taken specifically for gradients. However, since they were interesting they have been included. The low turbulence conditions during the night may shorten the time required to obtain a significant profile. The data based on the longer time periods indicated dry deposition of NO_x without exception. Some of the shorter periods indicate the ground as a source of NO_x but the short averaging time limits the application of the flux model and the gradient is of the same order as the 1% profile accuracy value. It is clear that little significance can be placed on the positive sign of these gradients.

Tables 22 to 24 show that the diffusivity values were limiting in all NO_x, NO and O_3 runs. The variation was so great that positive and negative values were nearly equally common. NO_x runs 4 and 5, all three NO runs, and most of the ozone runs had gradients that appear to be significant. These may yield further information with parameterization of the eddy diffusivity values in subsequent analysis. Considering the large experimental error, little significance can be placed on most of the computed deposition velocities in these tables. One exception is the NO runs where the relative errors are lowest.

All three NO runs have gradients that indicate significant deposition is occurring. The middle levels are felt to be the best for estimating the diffusivity for these runs. In the NO runs 2 and 3 (Table 23) the use of upper level momentum flux values produced negative diffusivities and the middle level positive diffusivities. Inspection of the meteorology summaries for the NO runs leads us to conclude that for these cases the constant flux surface layer is below the upper level and the middle level data are more appropriate. This produces deposition velocities for NO in the range of 0.08 to 0.12 cm/s. A low level of confidence in these numbers is primarily a function of the accuracy of the eddy diffusivity determination. The relative errors show only small changes based on several values of assumed profile accuracy.

With the limited size of the current data a definitive resolution of the accuracy of the pollutant profile is not possible. The listed accuracy of the gas concentrations is not claimed to be obtained in an absolute sense, but rather is stated to study the relative accuracy obtained by consideration of the profiles. The vertical consistency of the profiles indicate that the relative accuracy is better than the absolute accuracy and is sufficient for deposition computations.

The accuracy of profiles and the turbulence is interrelated. Small vertical pollutant gradients may be expected under greater turbulence. Pollutant gradients which are not significantly different from zero do not necessarily imply a zero flux. We have attempted to show this in the error analysis. That is, the range of possible values for the deposition velocity may be significantly non-zero. If it is not, then the measurements are implying a near zero flux to the surface. The computed ranges for deposition velocities do generally include the reasonable range of values that might be expected for the deposition velocity, and in cases where the computed range is narrow the magnitude of the deposition velocity is reasonable in most cases.

SECTION X

REFERENCES

1 Thom, A.S., J. B. Stewart, H. R. Oliver, and J. H. C. Gash. Comparison of Aerodynamic and Energy Budget Estimates of Fluxes over a Pine Forest. Quart. J. R. Meteor. Soc. 101: 93-105, 1975.

2 Aylor, D. E. Deposition of Particles in a Plant Canopy. J. Appl. Meteorol. 14: 52-57, 1975.

3 Bolin, B., G. Aspling, and C. Persson. Residence Time of Atmospheric Pollutants as Dependent on Source Characteristics, Atmospheric Diffusion Processes and Sink Mechanisms. Tellus 24: 1-2, 1974.

4 Scriven, R. A. and B. E. A. Fisher. The Long Range Transport of Airborne Material and Its Removal by Deposition and Washout - I. General Considerations, II. The Effect of Turbulent Diffusion. Atmos. Environ. 9: 49-58. 1975.

5 Hosker, Jr., R. P. Estimates of Dry Deposition and Plume Depletion over Forest and Grassland. (Presented at IAEA Symposium on the Physical Behavior of Radioactive Contaminants in the Atmosphere. Vienna. November 12-16, 1973).

6 Angeletti, L. La Contamination Des Paturages par L'iode-131 l'ere Purtie: Vitesse de Depot de L'iode-131. EUR-4872. (In French).

7 Droppo, J. G. Dry Deposition Processes on Vegetation Canopies. Proc. Atmosphere-Surface Exchange Particulate and Gaseous Pollutants - 1974 Symposium. Richland, WA. Septebmer 4-6, 1974. ERDA Symposium Series 38. CONF-740 921.

8 Hill, A. C. Vegetation: A Sink for Atmospheric Pollutants. J. Air Pollu. Con. Assoc. 21(6): 341-346, June 1971.

9 Garland, J. A. Dry Deposition of SO_2 and Other Gases . Proc. Atmosphere-Surface Exchange Particulate and Gaseous Pollutants - 1974 Symposium. Richland, WA. September 4-6, 1974. ERDA Symposium Series 38. CONF-740 921.

10 Slinn, W. G. N. Atmospheric Aerosols: Sources, Concentrations and Budgets. Proc. Atmosphere-Surface Exchange Particulate and Gaseous Pollutants - 1974 Symposium. Richland, WA. September 4-6, 1974. ERDA Symposium Series 38. CONF-740-921.

11 Hicks, B. B. Some Micrometeorological Aspects of Pollutant Deposition Rates Near the Surface. Proc. Atmosphere-Surface Exchange Particulate and Gaseous Pollutants - 1974 Symposium. Richland, WA. September 4-6, 1974. CONF-740-921

12 Bennett, J. H., A. C. Hill, and D. M. Gates. A Model for Gaseous Pollutant Sorption by Leaves. J. Air Pollu. Con. Assoc. 23(11): 957-962, November 1973.

13 Rasmussen, K. H., M. Taheri, and R. L. Kabel. Sources and Natural Removal Processes for Some Atmospheric Pollutants. Center for Air Environ. Studies. Penn State University. June 1974. EPA-650/4-74-032.

14 Select Research Group in Air Pollution Meteorology. Second Annual Progress Report: Volume II. Penn. State University. Grant No. R-800397. Office of Research and Development, Environmental Protection Agency, Washington, D.C. PB-241 391, EPA-650/4-74-045-6. September 1974.

15 deCormis, L. Some Aspects of Sulfur Absorption by Plants Subjected to an Atmosphere Containing SO_2. Proc. Air Pollution First European Congress. Netherlands. 1968.

16 Chamberlain, A. C. and R. C. Chadwick. Deposition of Airborne Radioiodine Vapor. Nucleonics 11(8): 22-25, August 1953.

17 Chamberlain, A. C. Aspects of the Deposition of Radioactive and Other Gases and Particles. Aerodynamic Capture of Particles. New York, Pergamon Press, 1960. p 63-68.

18 Chamberlain, A. C. Transport of Gases to and from Grass and Grass-like Surfaces. Proc. Roy. Soc. (A) London. 290: 236-265, 1966.

19 Chamberlain, A. C. and R. C. Chadwick. Transport of Iodine from Atmosphere to Ground. Tellus 18: 226-237, 1966.

20 Owen, P. R. and W. R. Thompson. Heat Transfer Areas Rough Surfaces. J. Fluid Mech. 15: 321, 1963.

21 Markee, Jr., E. H. Studies of the Transfer of Radioiodine Gas to and from Natural Surfaces. Environmental Research Laboratories, Air Resources Laboratories, Silver Spring, MD. April 1971. ERL-ARL-29.

22 Bunch, D. F. Controlled Environmental Radioiodine Tests (CERT), Progress Report No. 2. AEC Operations Office, Idaho Falls, ID. IDO-12053. 1966. p. 33ff.

23 Bunch, D. F. Controlled Environmental Radioiodine Tests (CERT), Progress Report No. 3. AEC Operations Office, Idaho Falls, ID. IDO-12063. 1968. p. 77ff.

24 Hawley, C. A. Controlled Environmental Radioiodine Tests (CERT) at NRTS, 1965 Progress Report. AEC Operations Office, Idaho Falls, ID. IDO-12047. 1966. p. 41ff.

25 Hawley, C. A., C. W. Sill, G. L. Voelz, and N. F. Islitzer. Controlled Environmental Radioiodine Tests (CERT) at NRTS. AEC Operations Office, Idaho Falls, ID. IDO-12035. 1964. p. 65ff.

26 Zimbrick, J. D. and P. G. Voilleque. Controlled Environmental Radioiodine Tests (CERT) at NRTS, Progress Report No. 4. AEC Operations Office, Idaho Falls, ID. IDO-12065. 1969. p. 78ff.

27 Garland, J. A., D. H. F. Atkins, C. J. Readings, and S. J. Cauhey. Technical Note: Deposition of Gaseous Sulphur Dioxide to the Ground. Atmos. Environ. 8: 75-79, 1974.

28 Owers, M. J. and A. W. Powell. Deposition Velocity of Sulfur Dioxide on Land and Water Surfaces Using a ^{35}C Tracer Method. Atmos. Environ. 8: 63-67, 1974.

29 Sheperd, J. G. Measurements of the Direct Deposition of Sulphur Dioxide onto Grass and Water by the Profile Method. Atmos. Environ. 8: 69-74, 1974.

30a Whelpdale, D. M. and R. W. Shaw. Sulphur Dioxide Removal by Turbulent Transfer over Grass, Snow and Water Surfaces. Tellus 26: 196-205, 1974.

30b Robinson, E. and R. C. Robbins. Gaseous Nitrogen Compound Pollutants from Urban and Natural Sources. J. Air Pollu. Con. Assoc. 20: 303-306, 1970.

31 Robinson, E. and R. C. Robbins. Sources, Abundance and Fate of Gaseous Atmospheric Pollutants. Final Report, SRI Project PR-6755. 1968.

32 Tingey, D. T. Foliar Absorption of Nitrogen Dioxide. Dept. of Botany, University of Utah. M.A. Thesis. 1968

33 Israel, G. W. Deposition Velocity of Gaseous Fluorides on Alfalfa. Atmos. Environ. 8: 1329-1330, 1974.

34 Kelley, Jr., J. J. and J. D. McTaggart Cowan. Vertical Gradient of Net Oxidant Near the Ground Surface at Barrow, Alaska. J. Geophys. Res. 73: 3328-3330, 1968.

35 Galbally, I. Ozone Variation and Destruction in the Amospheric Surface Layer. Nature, 218: 456-457. 1968.

36 Galbally, I. Evaluation of the Ehmert Technique for Measuring Ozone Profiles in the Atmospheric Surface Layer. J. Geophys. Res. 74: 6869-6872. 1968.

37 Aldaz, L. Flux Measurements of Atmospheric Ozone Near Land and Water. J. Geophys. Res. 74: 6934-6946. 1969.

38 Regener, V. H. and L. Aldaz. Turbulent Transport Near the Ground as Determined from Measurements of the Ozone Flux and the Ozone Gradient. J. Geophys. Res. 74: 6935-6942, 1969.

39 Galbally, I. Ozone Profiles and Ozone Fluxes in the Atmospheric Surface Layer. Quart. J. R. Meteor. Soc. 97: 18-29, 1971.

40 Megaw, W. J. and R. C. Chadwick. Some Field Experiments on the Release and Deposition of Fission Products and Thoria. AERE-HP-M-114. December 1956.

41 Convair. Fission Products Field Release Test I. Air Force Nuclear Aircraft Research Facility. AFSWC-TR-59-44. 1959.

42 Fission Products Field Release Test II. Air Force Nuclear Aircraft Research Facility. AFSWC-TR-60-26. 1960.

43 Slade, D. H. Meteorology and Atomic Energy 1968. U.S. Dept. of Commerce, Springfield, VA. TID-24190. 1968.

44 Servant, J. Deposition of Atmospheric Lead Particles to Natural Surfaces in Field Experiments. Proc. Atmosphere-Surface Exchange Particulate and Gaseous Pollutants - 1974 Symposium. Richland, WA. September 4-6, 1974. ERDA Symposium Series 38. CONF-740 921.

45 Cawse, P. A. and D. H. Peirson. An Analytical Study of Trace Elements in the Atmospheric Environment. AERE-R-7134. 1972.

46 Simpson, C. L. Some Measurements of the Deposition of Matter and Its Relation to Diffusion from a Continuous Point Source in a Stable Atmosphere. General Electric, Richland, WA. HW-69292 REV. April 1961.

47 Islitzer, N. F. and R. K. Dumbauld. Atmospheric Diffusion-Deposition Studies over Flat Terrain. Intern. J. Air Water Pollution. 7(11-12): 999-1022, 1963.

48 Whelpdale, D. M. Dry Deposition over the Great Lakes. Proc. Atmosphere-Surface Exchange Particulate and Gaseous Pollutants - 1974 Symposium. Richland, WA. September 4-6, 1974. ERDA Symposium Series 38. CONF-740 921.

49 Atmosphere-Surface Exchange of Particulate and Gaseous Pollutants. Oak Ridge, Division of Technical Information Exchange, 1974. 988 p. CONF-740 921.

50 Gifford, F. A. and D. H. Pack. Surface Deposition of Airborne Material. Nuclear Safety. 3(4): June 1962. p. 76ff.

51 Nickola, P. W. and G. H. Clark. Measurement of Particulate Plume Depletion by Comparison with Inert Gas Plumes. Pacific Northwest Laboratory Annual Report for 1973 to the USAEC Division of Biomedical and Environmental Research, Part 3: Atmospheric Sciences. BNWL-1850 PT3, Battelle, Pacific Northwest Laboratories, Richland, WA, April 1974. pp. 49-60.

52 Small, S. H. Wet and Dry Deposition of Fallout Materials at Kjeller. Tellus. 12: 308-314, 1960.

53 Marenco, A. and J. Fontan. Influence of Dry Deposition on Residence Time in Troposphere of Particulate Pollutants. Proc. Atmosphere-Surface Exchange Particulate and Gaseous Pollutants - 1974 Symposium. Richland, WA. September 4-6, 1974. ERDA Symposium Series 38. CONF-740 921.

54 Sehmel, G. A. Turbulent Deposition of Monodispersed Particles on Simulated Grass. II. Assessment of Airborne Particles. Springfield, C. Thomas Publishing Company. 1972. pp. 18-42.

55 Sehmel, G. A. and S. L. Sutter. Particle Deposition Rates on a Water Surface as a Function of Particle Diameter and Air Velocity. Pacific Northwest Laboratory Annual Report for 1973 to the USAEC Division of Biomedical and Environmental Research, Part 3: Atmospheric Sciences. BNWL-1850 PT3, Battelle, Pacific Northwest Laboratories, Richland, WA, April 1974. pp. 171-174.

56 Sehmel, G. A. and W. H. Hodgson. Particle and Gaseous Removal in the Atmosphere by Dry Deposition. Proc. Symposium on Atmospheric Diffusion and Air Pollution, Santa Barbara, CA, September 9-13, 1974.

57 Sehmel, G. A. and W. H. Hodgson. Particle Dry Deposition Velocities. Proc. Atmosphere-Surface Exchange Particulate and Gaseous Pollutants - 1974 Symposium. Richland, WA. September 4-6, 1974. ERDA Symposium Series 38. CONF-740 921.

58 Hicks, B. B. Transfer of SO_2 and Other Reactive Gases Across the Air-Sea Interface. (To be published in Tellus).

59 Heinemann, K. and K. J. Vogt. Deposition and Biological Heat-Life of Elemental Iodine on Grass and Clover. Proc. Atmosphere-Surface Exchange Particulate and Gaseous Pollutants - 1974 Symposium. Richland, WA. September 4-6, 1974. ERDA Symposium Series 38. CONF-740 921.

60 Pyatt, F. B. Plant Sulphur Content as an Air Pollution Gauge in the Vicinities of Steelworks. Envirn. Pollut. 5: 103-115, 1973.

61 Martin, A. and F. Barber. Some Measurements of Loss of Atmospheric Sulphur Dioxide Near Foliage. Atmos. Environ. 5: 345-352, 1971.

62 Mansfield, T. A. and O. V. S. Heath. An Effect of "Smog" on Stomatal Behavior. Nature (London). 200: 596, 1963.

63 Spedding, D. J. Uptake of Sulfur Dioxide by Barley Leaves at Low Sulfur Dioxide Concentrations. Nature. 224: 1229-1231, 1969.

64 Majernik, O. and T. A. Mansfield. Stomatal Responses to Raised Atmospheric CO_2 Concentrations During Exposure of Plants to SO_2 Pollution. Environ. Pollut. 3:1-7, 1972.

65 Abeles, F. B., L. E. Craker, L. E. Forrence, and G. R. Leather. Fate of Air Pollutants. Removal of Ethylene, Sulfur Dioxide and Nitrogen Dioxide by Soil. Science. 173:(4000). 914-916, 1971.

66 Bennett, J. H. and A. C. Hill. Absorption of Gaseous Air Pollutants by a Standardized Plant Canopy. J. Air Pollut. Control Assoc. 23:203-206, 1973.

67 Liss, P. S. Exchange of SO_2 Between the Atmosphere and Natural Waters. Nature. 233:327-329, 1971.

68 Liss, P. S. and P. G. Slater. Flux of Gases Across the Air-Sea Interface. Nature. 247:181-184, 1974.

69 Hales, J. M. and S. L. Sutter. Solubility of Sulfur Dioxide in Water at Low Concentrations. Atmos. Environ. 7:997-1001, 1973.

70 Spedding, D. J. SO_2 Uptake by Limestone. Atmos. Environ. 3:683, 1969.

71 Spedding, D. J. Sulfur Dioxide Absorption by Sea Water. Atmos. Environ. 6:583-586, 1972.

72 Payrissat, M. and S. Beilke. Laboratory Measurements of the Uptake of Sulfur Dioxide by Different European Soils. Atmos. Environ. 9:211-217, 1975.

73 Fisher, B. E. A. Discussion of Reference 72. Atmos. Environ. 9:553, 1975.

74 Smith, K. A., J. M. Bremer, and M. A. Tabatabai. Sorption of Gaseous Atmospheric Pollutants by Soils. Soil Science. 116(4):313-319, 1973.

75 Terraglio, F. P. and R. M. Manganelli. The Influence of Moisture on the Adsorption of Atmospheric SO_2 by Soil. Int. J. Air & Water Poll. 783-791, November-December 1966.

76 Horst, T. W. A Surface Flux Model for Diffusion, Deposition, and Resuspension. Pacific Northwest Laboratory Annual Report for 1973 to the USAEC Division of Biomedical and Environmental Research, Part 3, Atmospheric Sciences. BNWL-1850 PT3. Battelle, Pacific Northwest Laboratories, Richland, WA, April 1974. pp. 63-67.

77 Elderkin, C. E., D. C. Powell, G. H. Clark, and P. W. Nickola. Comparison of Diffusion-Deposition Model Components with Experimental Results. Pacific Northwest Laboratory Annual Report for 1973 to the USAEC Division of Biomedical and Environmental Research, Part 3, Atmospheric Sciences. BNWL-1850 PT3. Battelle, Pacific Northwest Laboratories, Richland, WA, April 1974. pp. 38-44.

78 Droppo, J. G. and J. M. Hales. Profile Methods of Dry Deposition Measurement. Proc. Atmosphere-Surface Exchange Particulate and Gaseous Pollutants - 1974 Symposium. Richland, WA, September 4-6, 1974. ERDA Symposium Series 38. CONF-740 921.

79 Hales, J. M., J. M. Thorp, and M. A. Wolf. Field Investigation of Sulfur Dioxide Washout from the Plume of a Large Coal-Fired Power Plant by Natural Precipitation. Final Report. Environmental Protection Agency No. CPA22-69-150. 1971.

80 Shaffer, W. A. Atmospheric Diffusion of Radon in a Time-Height Regime. Ph.D. Thesis. Drexel University. June 1973.

81 Pasquill, F. Atmospheric Diffusion, 2nd Edition. New York. John Wiley & Sons. 1974.

82 Pearman, G. I. and J. R. Garrett. Carbon Dioxide Measurements Above a Wheat Crop. 1. Observations of Vertical Gradients and Concentrations. Agr. Meteor. 12: 13-25, 1973.

83 Zlatkis, A., H. A. Lichtenstein, A. Tishbee. Concentrations and Analysis of Trace Volatile Organics in Gases and Biological Fluids with a New Solid Adsorbent. Chromatographia. 6:67, 1973.

84 Droppo, J. G. and H. L. Hamilton. Experimental Variability in the Determination of the Energy Balance in a Deciduous Forest. J. Appl. Meteor. 12(5):781-791, August 1973.

85 Paulson, C. A. Profiles of Wind Speed, Temperature and Humidity Over the Sea. Ph.D. Thesis, University of Washington, Seattle, Washington.

86 Gill, G. C. Development and Use of the Gill UVW Anemometer. Proc. 3rd Symposium on Meteorology and Observations and Transformation. Washington, DC. February 10-13, 1974.

87 Horst, T. W. Corrections for Response Errors in a Three-dimensional Propellor Anemometer. J. Appl. Meteor. 12:716-725, 1973.

88 Garratt, J. R. Limitations of the Eddy-Correlation Technique for the Determination of Turbulent Fluxes Near the Surface. Boundary-Layer Meteorology. 8:255-259, 1975.

89 Whelpdale, D. M. and R. W. Shaw. Sulphur Dioxide Removal by Turbulent Transfer Over Grass, Snow, and Water Surfaces. Tellus. 24:1-2, 1974.

SECTION XI

NOMENCLATURE

Units: L = length; m = mass; t = time; °C = °C;
°A = °A; units = as defined by quantity
of interest; none = nondimensional;
E = energy.

Symbol	Units	Definition
B	units	"y" intersect in least squares fit
B^{-1}	none	Stanton number
C_p	$E\ M^{-1}\,{}^{\circ}A^{-1}$	Specific heat at constant pressure for air
D	$t\ L^{-2}$	Diffusion function
f	L^{-1}	Gradient factor
G	$L^{-2}t^{-1}$	Flux to surface
h	L	Release height
K	$L^{2}t^{-1}$	Eddy diffusivity
K_m	$L^{2}t^{-1}$	Eddy diffusivity for momentum
K_h	$L^{2}t^{-1}$	Eddy diffusivity for heat
K_o	$L^{2}t^{-1}$	Eddy diffusivity for water vapor
L	$E\ M^{-1}$	Latent heat for evaporation of water
m	units	Slope in least squares fit
Q	t^{-1}	Source strength
q	none	Specific humidity
T	°C	Air temperature
u	$L\ t^{-1}$	Wind speed

w	$L\ t^{-1}$	Vertical velocity
x	L	Downwind distance
Ri	none	Richardson number
z	L	Height
$(')$	units	Indicates departure from mean value
$(\bar{\ })$	units	Indicates mean value
r_a	$t\ L^{-1}$	Atmospheric resistance
r_g	$t\ L^{-1}$	Gravitational resistance
r_i	$t\ L^{-1}$	Internal resistance
r_ℓ	$t\ L^{-1}$	Surface layer resistance
r_s	$t\ L^{-1}$	Effective surface layer resistance
r_T	$t\ L^{-1}$	Total resistance
r_τ	$t\ L^{-1}$	Momentum flux resistance
v_d	$L\ t^{-1}$	Deposition velocity
v_s	$L\ t^{-1}$	Settling velocity
χ	units L^{-3}	Air concentration
ρ	$M\ L^{-3}$	Density of air
$\sigma_{(\ )}$	units	Standard deviation of variable
Θ	°A	Potential temperature
ξ	L	Downwind surface source coordinate

SECTION XII

APPENDICES

Page

A. NUCLEPORE FILTER ANALYSIS RESULTS FROM ORTEC 107

B. NUCLEPORE FILTER ANALYSIS RESULTS FROM BATTELLE COLUMBUS LABORATORIES 121

APPENDIX A

NUCLEPORE FILTER ANALYSIS RESULTS FROM ORTEC

HIGH PRECISION ENERGY DISPERSIVE X-RAY FLUORESCENCE ANALYSIS of SULFUR IN AEROSOLS DEPOSITED ON FILTER PAPERS

By

JOHN A. COOPER
ORTEC, Incorporated
100 Midland Road
Oak Ridge, Tennessee 37830

September 11, 1975

HIGH PRECISION ENERGY DISPERSIVE X-RAY FLUORESCENCE ANALYSIS OF SULFUR IN AEROSOLS DEPOSITED ON FILTER PAPER

John A. Cooper
ORTEC, Incorporated
100 Midland Rd.
Oak Ridge, Tennessee 37830

September 11, 1975

INTRODUCTION

Dry deposition of atmospheric aerosols is a significant mechanism for removal of atmospheric contaminants which may exceed precipitation scavenging under some climatological conditions. The development of a reliable model for predicting the contribution of dry deposition to the removal of material from fossil fuel power plant effluents by profile measurement techniques requires accurate determination of small differences (a few percent) in chemical composition as a function of altitude. These differential composition measurements require both accurate sampling procedures and precise analytical methods.

This investigation is part of a larger study which includes the collection of aerosol and gaseous samples at different altitudes and the measurement of the vertical profile for the gaseous components CO, NO, NO_2, H_2S, SO_2, O_3, hydrocarbons as well as $SO_4^=$, NO_2^-, NO_3^- and organic particulates. The purpose of this part of the study is to develop a precise method for the analysis of S in aerosols deposited on filter paper by energy dispersive x-ray fluorescence analysis and to analyze a series of aersol sample collected at different altitudes.

THEORETICAL CONSIDERATIONS

Energy dispersive x-ray fluorescence analysis of S in aerosols is complicated by spectral interferences and uncertainties due to x-ray absorption in the collection filters and deposited particulate material.

Sulphur emits a 2.31 keV K x-ray which may be spectrally interferred with by unresolved Mo L line at 2.29 keV and a Pb M line at 2.35 keV. The Mo L line is not a common interference in aerosol analyses because of its low abundance. Lead, however, is typically as abundant as S (Figure 1) and must be corrected for in any S analysis.

The analysis procedure used in this study included measurements of the Pb and Mo concentration in each filter and the correction of the

2.3 keV x-ray peak intensity for the presence of Pb. (Mo was not corrected for because of its consistently low levels.)

Accurate analysis of S in deposited aerosols will also require corrections for x-ray absorption in the filter and the deposited particulates. The magnitude of these errors, however, is small for this study because of the interest in relative concentration differences. Errors associated with the sample would thus be caused mainly by differences in significant particle size distributions and/or differences in deposition patterns in addition to obvious uncertainties in air volumes sampled per unit filter area.

EXPERIMENTAL CONDITIONS

Sample Description

The samples analyzed consisted of aerosols deposited on Nuclepore filters. The filter diameter was about 1 3/4 inches in diameter while the exposed area was only 1 1/4 inches. The exposed area represents a collection of about 5 cfm over a period of about one hour.

The samples were received in labeled plastic pill boxes. It appeared as though the aerosol was deposited on the dull side of the filter. Standards prepared by Columbia Scientific Inc., by depositing known amounts of material in solution form on millipore filters were used to determine the relative counting rates for Pb using the L and M lines and estimating the absolute counting rates of Pb and S.

A piece of Nuclepore filter from a different batch was used as a blank. The S standard contained 75 $\mu g/cm^2$ of elemental S while the Pb standard contained 24 $\mu g/cm^2$.

Sample Preparation

The filters were taped to 2 inch diameter flat plastic rings with the dull side of the filter exposed to the x-ray tube and detector. The plastic holders were mounted in an Al wheel with a positioning accuracy of ±.002 in between the x-ray tube-sample and sample-tube distance.

Instrumentation

An ORTEC Model 6110 Tube Excited Fluorescence Analyzer was used for the analysis. The samples were analyzed in vacuum with the excitation conditions listed in Table 1.

TABLE 1

Anode	Filter	Voltage (KV)	Current (UA)
Mo	--	10	200
W	--	10	200
W	--	15	200
W	Al	15	200
Mo	Mo(3)	40	200

Software

The samples were analyzed automatically using the intensity-only version of the XRFCALC program which determines the net x-ray intensities above background for each element defined with a region of interest.

RESULTS

The major elemental components (Al, Si, S (Pb), Cl, K, Ca and Fe) present in the aerosol samples are illustrated with the low energy x-ray spectra of Sample M7-1 shown in Figures 1 to 3. Low intensity peaks associated with Na, Mg, P and Ti were also observed. Figures 1 and 2 contrasts the differences between spectra excited with filtered and unfiltered radiation from a W anode.

The high energy portion of the x-ray spectra are illustrated in Figures 3 to 6 which show the clear presence of Fe, Ni, Cu, Zn, Pb and Br. The logarithmic plot shown in Figure 4 is contrasted with the linear plot in Figure 5 and the spectra of an unrelated rural aerosol shown in Figure 6.

A spectrum of scattered radiation off the plastic sample holder is shown in Figure 7 and illustrates the low system blank.

The samples were analyzed eight times under several different excitation conditions and each sample was rotated between analysis. The averages from these analyses are listed along with expected errors in Table 2.

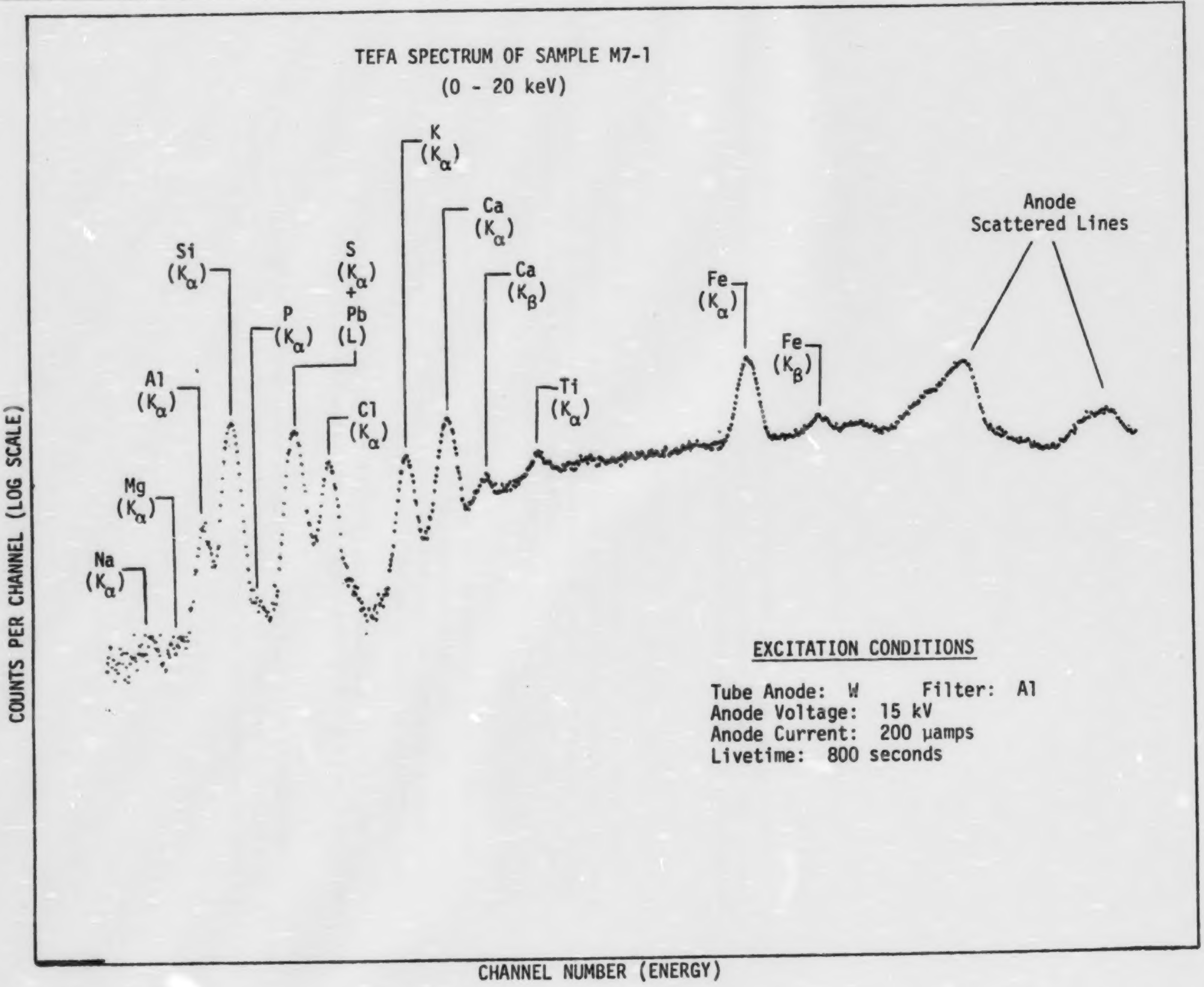
TEFA SPECTRUM OF SAMPLE M7-1
(0 - 20 keV)
Na (K_α)
Mg (K_α)
Al (K_α)
Si (K_α)
P (K_α)
S (K_α) + Pb (L)
Cl (K_α)
K (K_α)
Ca (K_α)
Ca (K_β)
Ti (K_α)
Fe (K_α)
Fe (K_β)
Anode Scattered Lines
EXCITATION CONDITIONS
Tube Anode: W Filter: Al
Anode Voltage: 15 kV
Anode Current: 200 µamps
Livetime: 800 seconds
COUNTS PER CHANNEL (LOG SCALE)
CHANNEL NUMBER (ENERGY)

Figure 1

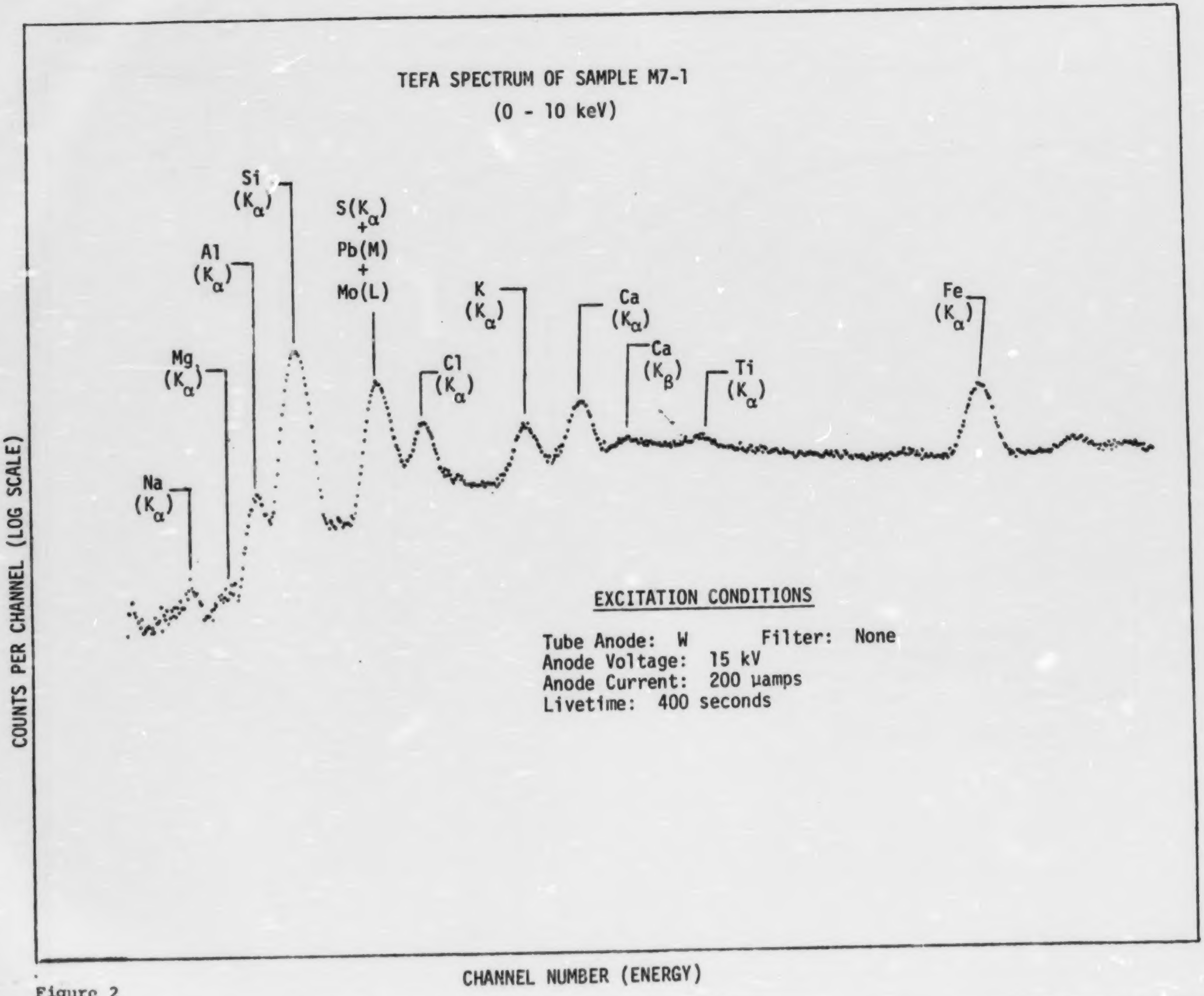
TEFA SPECTRUM OF SAMPLE M7-1

(0 - 10 keV)

EXCITATION CONDITIONS

Tube Anode: W Filter: None
Anode Voltage: 15 kV
Anode Current: 200 µamps
Livetime: 400 seconds

Figure 2

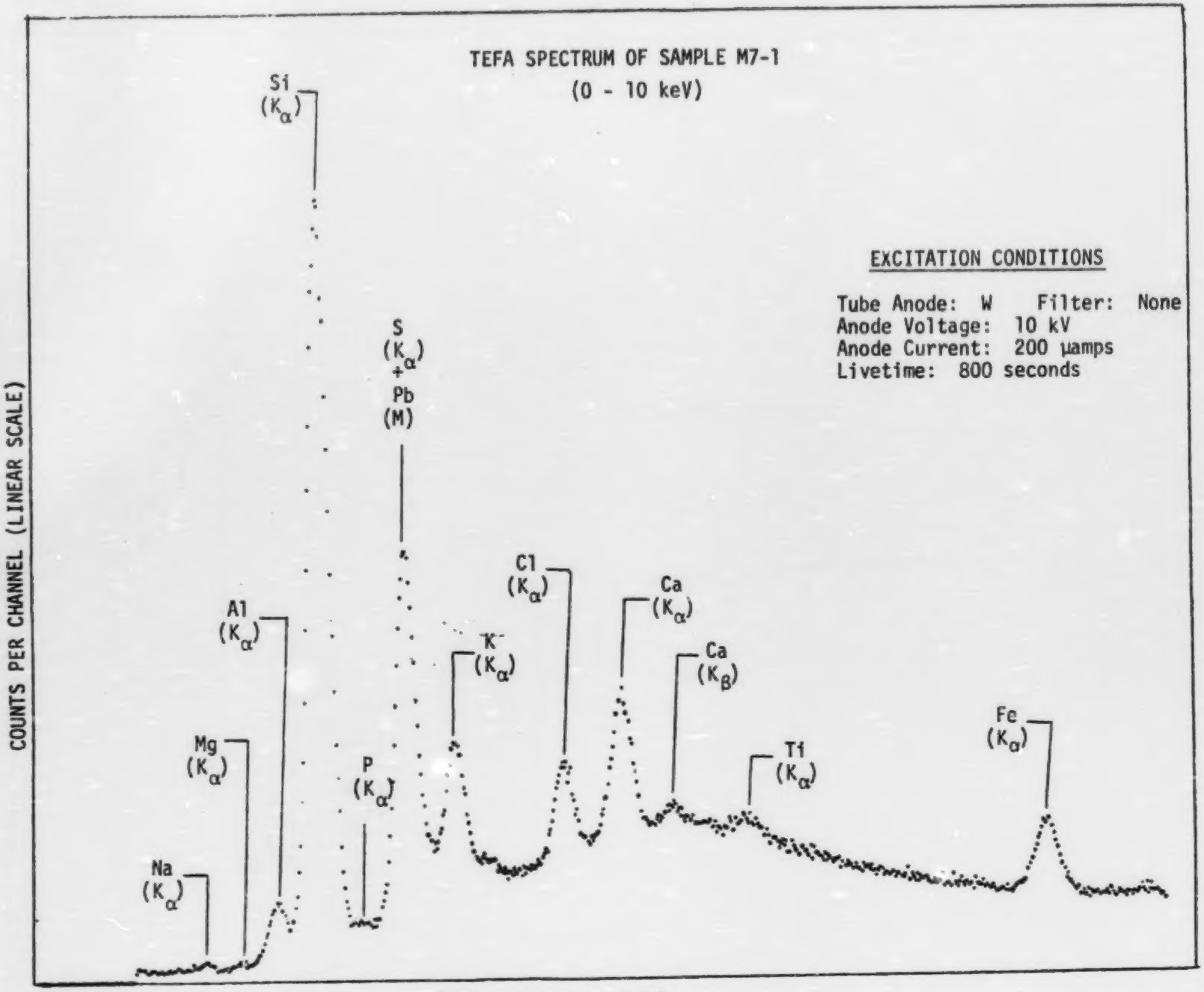
TEFA SPECTRUM OF SAMPLE M7-1
(0 - 10 keV)
EXCITATION CONDITIONS
Tube Anode: W Filter: None
Anode Voltage: 10 kV
Anode Current: 200 µamps
Livetime: 800 seconds
Si (K_α)
S (K_α) + Pb (M)
Al (K_α)
Mg (K_α)
Na (K_α)
P (K_α)
K (K_α)
Cl (K_α)
Ca (K_α)
Ca (K_β)
Ti (K_α)
Fe (K_α)
COUNTS PER CHANNEL (LINEAR SCALE)
CHANNEL NUMBER (ENERGY)

Figure 3

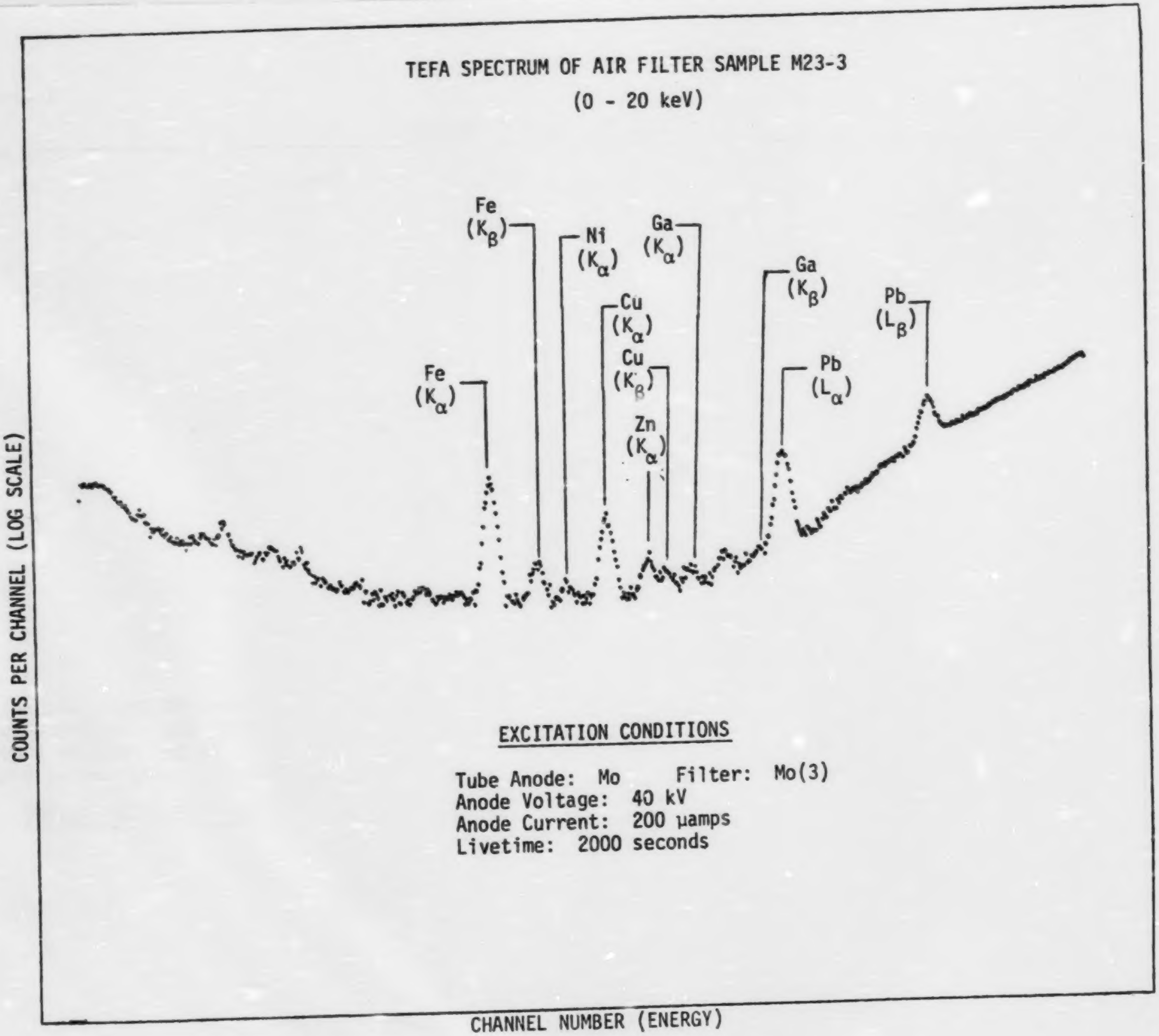
TEFA SPECTRUM OF AIR FILTER SAMPLE M23-3
(0 - 20 keV)
Fe (K_α)
Fe (K_β)
Ni (K_α)
Cu (K_α)
Cu (K_β)
Zn (K_α)
Ga (K_α)
Ga (K_β)
Pb (L_α)
Pb (L_β)
COUNTS PER CHANNEL (LOG SCALE)
CHANNEL NUMBER (ENERGY)
EXCITATION CONDITIONS
Tube Anode: Mo Filter: Mo(3)
Anode Voltage: 40 kV
Anode Current: 200 µamps
Livetime: 2000 seconds

Figure 4

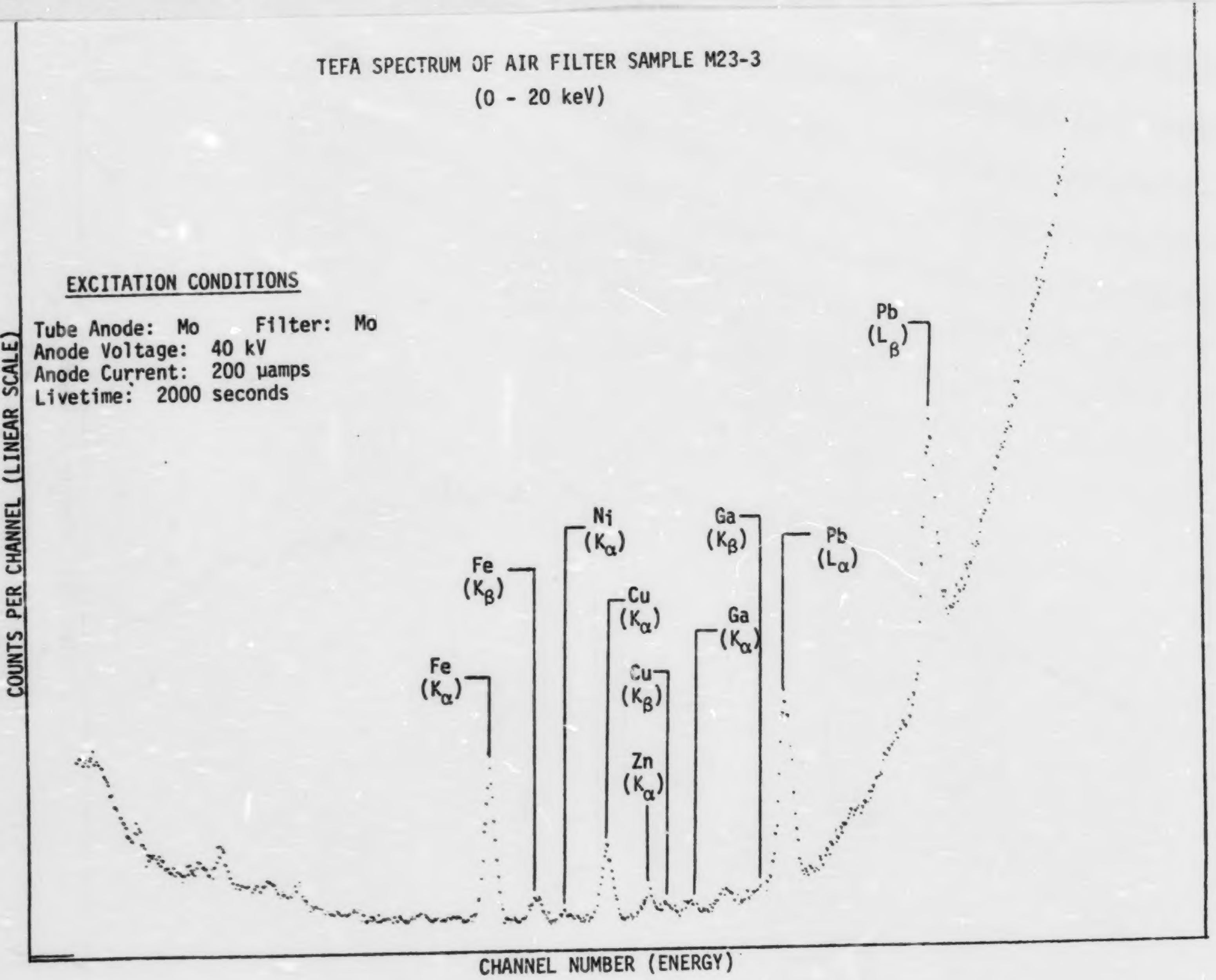
TEFA SPECTRUM OF AIR FILTER SAMPLE M23-3

(0 - 20 keV)

EXCITATION CONDITIONS

Tube Anode: Mo Filter: Mo
Anode Voltage: 40 kV
Anode Current: 200 μamps
Livetime: 2000 seconds

Figure 5

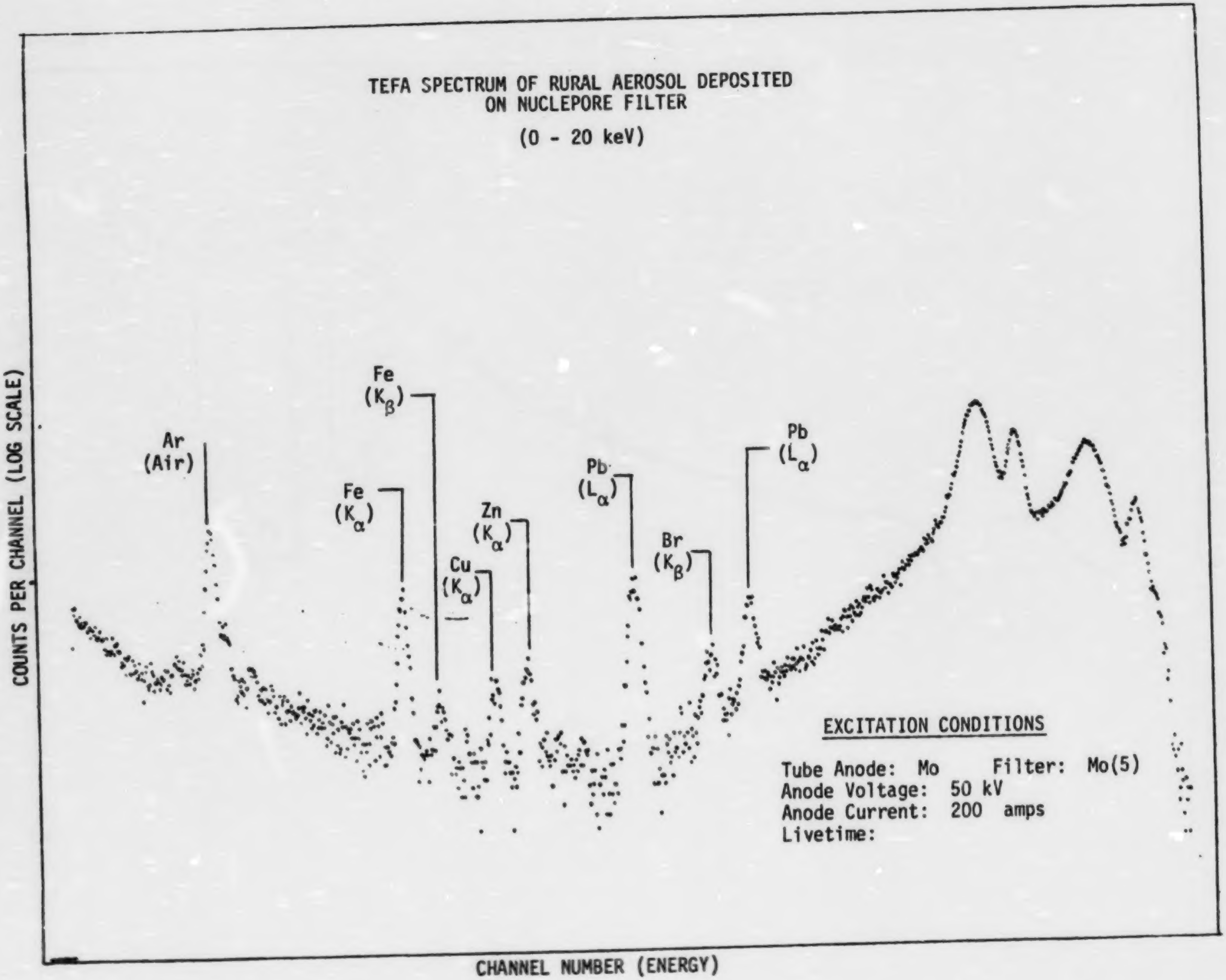
TEFA SPECTRUM OF RURAL AEROSOL DEPOSITED
ON NUCLEPORE FILTER
(0 - 20 keV)
Ar (Air)
Fe (K_α)
Fe (K_β)
Cu (K_α)
Zn (K_α)
Pb (L_α)
Br (K_β)
Pb (L_α)
EXCITATION CONDITIONS
Tube Anode: Mo
Filter: Mo(5)
Anode Voltage: 50 kV
Anode Current: 200 amps
Livetime:
COUNTS PER CHANNEL (LOG SCALE)
CHANNEL NUMBER (ENERGY)

Figure6

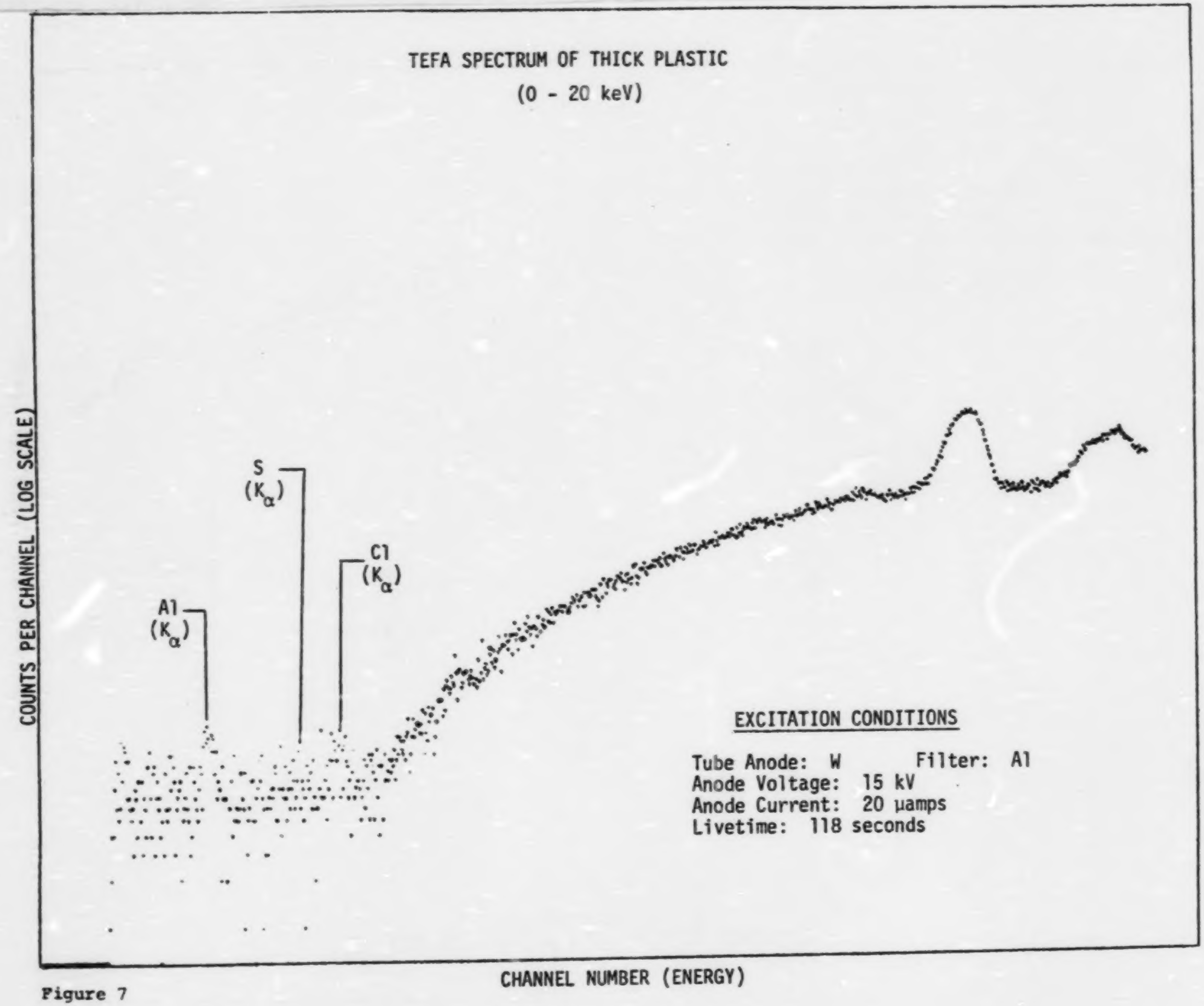

TEFA SPECTRUM OF THICK PLASTIC

(0 - 20 keV)

EXCITATION CONDITIONS

Tube Anode: W Filter: Al
Anode Voltage: 15 kV
Anode Current: 20 µamps
Livetime: 118 seconds

Figure 7

TABLE 2

AVERAGE SULPHUR AND LEAD CONCENTRATIONS ON NUCLEPORE FILTERS AND RELATIVE CHANGE IN SULPHUR CONCENTRATIONS

Sample No.	Number of S Analyses	Average S * Conc. (ug/cm^2)	Average Relative Change in S Conc.	Pb Conc. (ug/cm^2)
1-3	10	1.43 ± .02	1.00	0.66 ± .02
1-20	10	1.27 ± .02	0.89 ± .02	0.47 ± .02
1-50	8	1.29 ± .02	0.90 ± .02	0.48 ± .02
M7-1	6	2.56 ± .04	1.00	0.67 ± .02
M7-2	6	2.18 ± .04	0.85 ± .02	0.62 ± .02
M7-3	5	2.25 ± .04	0.88 ± .02	0.62 ± .02
M8-1	9	3.02 ± .05	1.00	0.59 ± .02
M8-2	9	2.79 ± .04	0.92 ± .02	0.59 ± .02
M8-3	9	2.81 ± .04	0.93 ± .02	0.57 ± .02
M12-1	10	2.64 ± .04	1.00	0.48 ± .02
M12-2	10	2.34 ± .04	0.89 ± .02	0.45 ± .02
M12-3	10	2.33 ± .04	0.88 ± .02	0.43 ± .01
M23-1	6	0.45 ± .01	1.00	0.50 ± .02
M23-2	6	0.46 ± .01	1.02 ± .02	0.38 ± .01
M23-3	6	0.41 ± .01	0.91 ± .02	0.35 ± .01

The errors listed in this table are precisional errors based upon repetitive analyses.

* This concentration will be low by a constant factor of about 20% due to differences in the deposition patterns between the standard and the specimens.

REFERENCES

1. Plesh, R. "X-Ray Fluorescence Analysis of Sulfur Precipitates on Air Filters" Siemans X-Ray Analytical Application Notes No. 12.

2. Bonnevie-Svendsen, M. and A. Follo, "Evaluation of filters, Standardization and Measuring Procedures for X-Ray Fluorescence Analysis of Sulphur in Air-Born Matter," Norwegian Institute for Nuclear Pnergy report number DH-98, June 1972.

3. Dzubay, T. G. and R. O. Nelson, "Self Absorption Corrections for X-Ray Fluorescence Analysis of Aerosols" Denver X-Ray Applications 1974

APPENDIX B

NUCLEPORE FILTER ANALYSIS RESULTS FROM BATTELLE COLUMBUS LABORATORIES

Battelle
Columbus Laboratories
505 King Avenue
Columbus, Ohio 43201
Telephone (614) 299-3151
Telex 24-5454

October 6, 1975

Dr. J. G. Droppo
Battelle, Pacific Northwest Laboratories
Battelle Boulevard
P.O. Box 999
Richland, Washington 99352

Dear Jim:

This letter confirms the results relayed to you earlier regarding the analyses of 15 nucleopore filter catches for sulfur. The conditions to be achieved in this effort were a total sulfur content determination having a precision of 1% and a quantitative estimate of about 20%. In addition, a direct comparison of the results were to be made after analyses of the same samples using energy-dispersion (ortec) in one case and wavelength dispersion (Battelle - Columbus) in the other.

The analyses were performed at Battelle using a conventional wavelength-type X-ray fluorescence unit. Sufficient counts were accumulated at the α sulfur peak to provide counting statistics of 1% for all samples. For the M-23 series, counting times of 400 seconds were necessary for the desired precision, where as for all other samples only 200 seconds were required.

Synthetic standards were prepared by drying appropriate amounts of an aqueous solution of Na_2SO_4 onto unused nucleopore filters. The prepared standards provided a linear working curve from 2 to 200 micrograms/$3cm^2$.

The results of these analyses are shown in Table 1 as total sulfur per active filter area ($\sim 11.4\ cm^2$). The condition of 1% percision among filter values appears to have been substantiated from a comparison of these and the preliminary Ortec data you have received. The accuracy of these analyses however is difficult to assess and may require complete filter destruction for analysis by some absolute method.

During our last phone conversation I mentioned attempting to determine the sulfur state on these catches using x-ray fluorescence. Sample M-8(1) was used for this investigation of the possible definitive variations of the sulfur peaks. The results of this examination indicated that sulfur was present solely as the sulfate. Also, the peak anomalies point toward calcium as the cation. Subsequent X-ray scan revealed that calcium is present in sufficient amounts that may approximate the sulfate molar concentration.

I want to thank you for successfully extending the project so that I could recover most of the costs. I still have the samples and will await word regarding their dispensation.

Please let me know if we can be of further service to you.

Very truly yours,

Ben Paris
Research Chemist
Analytical and Physical Chemistry Section

BP:lj

Enc: 1 Table

TABLE 1. TOTAL SULFUR CONTENT OF NUCLEOPORE FILTER CATCHES
(Results in total micrograms)

Sample		Total S
5/12/75	3 feet (1)	4.2
	20 feet (2)	3.8
	50 feet (3)	4.0
5/13/75	M-7 (1)	7.4
	M-7 (2)	6.4
	M-7 (3)	6.7
	M-8 (1)	8.2
	M-8 (2)	7.8
	M-8 (3)	7.6
5/14/75	M-12 (1)	7.4
	M-12 (2)	6.7
	M-12 (3)	6.7
5/16/75	M-23 (1)	2.1
	M-23 (2)	2.1
	M-23 (3)	1.9